Radar Systems for the Water Resources Mission - Final Report

RSL Technical Report 295-3
Vol. III

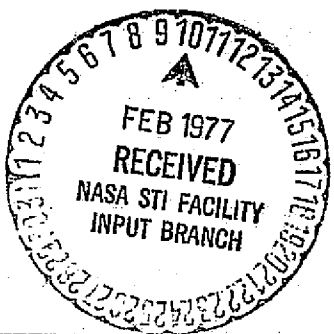

THE UNIVERSITY OF KANSAS CENTER FOR RESEARCH, INC.
2291 Irving Hill Drive—Campus West Lawrence, Kansas 66045

THE UNIVERSITY OF KANSAS SPACE TECHNOLOGY CENTER
Raymond Nichols Hall
2291 Irving Hill Drive—Campus West Lawrence, Kansas 66045

Telephone:

RADAR SYSTEMS FOR THE WATER RESOURCES MISSION
FINAL REPORT

Remote Sensing Laboratory
RSL Technocal Report 295-3
Volume III

R. K. Moore
J. P. Claassen
R. L. Erickson
R. K. T. Fong
B. C. Hanson
M. J. Komen
S. B. McMillan
S. K. Parashar

June, 1976

Supported by:

NATIONAL AERONAUTICS AND SPACE ADMINISTRATION
Goddard Space Flight Center
Greenbelt, Maryland 20771

CONTRACT NAS 5-22384

Technical Monitor: Dr. James Shiue

VOLUME III TABLE OF CONTENTS

APPENDIX A

RSL TECHNICAL REPORT 295-3

VOLUME III

THE UNIVERSITY OF KANSAS SPACE TECHNOLOGY CENTER
Raymond Nichols Hall
2291 Irving Hill Drive—Campus West Lawrence, Kansas 66045

Telephone:

RADAR AND RADIOMETER MEASUREMENT OF SOIL MOISTURE — STATE OF THE ART

Remote Sensing Laboratory
RSL Technical Memorandum 295-6

Brad Hanson

March, 1976

Supported by:

NATIONAL AERONAUTICS AND SPACE ADMINISTRATION
Goddard Space Flight Center
Greenbelt, Maryland 20771

CONTRACT NAS 5-22384

TABLE OF CONTENTS

LIST OF TABLES

LIST OF FIGURES

ABSTRACT

Radar offers promise of orbital monitoring of near-surface soil moisture. The complex dielectric constant affords an excellent estimate of the soil moisture content due to its dependence of the free water content in the soil. Target composition dictates the complex dielectric constant while surface roughness is characteristic of surface and to some degree sub-surface composition. By varying any one of the controllable parameters of a radar system (incidence angle, polarization, frequency) it is possible to measure the effects of surface roughness and dielectric constant from the standpoint of returned power. The effect of roughness on the radar backscattering coefficient, σ^o, can be minimized by the proper choice of the radar parameters without any significant reduction in the sensitivity to variations in soil moisture. Soil moisture is a greatly fluctuating entity and therefore monitoring must be performed relatively often and with realistic sensor instrumentation to insure optimum data retrieval. The following recommendations are submitted:

angle of incidence range:	7^o to 15^o
frequency:	4 GHz
polarization:	HH or VV
revisit time:	4 days
resolution:	100 meters

RADAR AND RADIOMETER MEASUREMENT OF SOIL MOISTURE -- STATE OF THE ART

Brad Hanson

1.0 INTRODUCTION

The surface layer of soil is of utmost importance to civilization. Maximizing cultivation output relies upon the maintenance of an optimum environment for this layer, a goal of cultivators for centuries. A key parameter in this environment is water but it has been only recently that changes in the soil water content for this surface zone have been understood [Jackson, 1973].

The purpose of this paper is to review recent work in the field of remote sensing relative to soil moisture, to recognize the target parameters necessary if optimum data retrieval is to be realized, and to recommend proper sensor instrumentation to achieve this goal.

2.0 PREVIOUS WORK

2.1 Passive Sensors

The primary concern to the hydrologist involved in large-scale, water resource management in farming regions is soil moisture; the method most actively utilized for data gathering lies in the realm of remote sensing. A number of investigations to determine soil moisture have been undertaken to determine the potential use of remote sensors which operate in the optical and thermal infrared regions of the electromagnetic spectrum [Luder, 1959; Gates, 1964; Stockhoff, 1971; Werner et al., 1971; and Reeves, 1973]. Their results reflect two major problems: cloud cover often hampered data retrieval and the sensor response at optical and infrared frequencies produced information relative to only a very thin layer at the air-soil interface.

Extensive research with passive microwave radiometers has been undertaken by many institutions including private industry, government agencies, and various universities.

Edgerton [1968] conducted experiments utilizing a microwave radiometer to ascertain its applicability for determining soil moisture. He noted that differences in emission could be measured from fields exhibiting variations in soil moisture conditions. Similar results were noted by Poe [1971]. Schmugge and others [1972] concluded that it was possible to monitor soil moisture from a radiometer mounted on an aircraft at the frequencies of 1.42 GHz, 4.99 GHz, 19.35 GHz, and 37 GHz. They noted, however, that the emissions were not only a function of soil moisture, but were affected by soil type and surface conditions such as roughness and vegetative cover. Experimentation by other research groups [Jean et al., 1972; Siu, 1974] substantiate the influence that soil moisture possesses on radiometric emissions.

There exist two major drawbacks which place severe limitations on an operational system for continuously monitoring soil moisture. Atmospheric effects such as cloud cover would severely limit or negate data, thus placing restrictions in some instances on the usefulness of the information retrieved. Achievable resolution is another problem. Edgerton [1968] and Poe [1971] noted that at satellite altitudes, soil moisture discrimination is practical only for gross spacial differences; at altitudes feasible from aircraft, the swath width involved is much too narrow. A similar problem was noted for a radiometric study over a Texas site [Sobti, 1975]. He concluded that while soil moisture has a substantial influence on the radiometric response, it is extremely difficult to predict soil moisture using the gross resolution sensors. It was noted, however, that it was feasible in a few instances to refine estimates where crude ones existed.

Operational constraints, both from the standpoint of system parameters and target response, severely limit the amount of useable data possible from passive microwave radiometers. Resolution is a major concern along with atmospheric restrictions such as cloud cover. It is the opinion of this investigator that launching an operational satellite system to monitor soil moisture with a passive microwave radiometer as the principle sensor would yield a limited amount of useable data. However, a satellite incorporating an active microwave sensor such as a radar plus a radiometer may lead to more information about a given target than if the latter system were eliminated from a satellite, sensor package.

2.2 Active Sensors

Active remote sensors such as radar are not restricted by the problems pre-

viously discussed. Radar is not hampered by non-precipitation clouds and depending upon frequency, surface as well as near-sub-surface moisture condition information is practical. Also, fine resolution imagery is achievable from any altitude since resolution is independent of range (fully focussed, synthetic-aperture radar).

Five parameters affect the reflection or scattering of electromagnetic waves from a target; they are polarization, frequency, incidence angle, complex dielectric constant and surface roughness. Of these parameters, the last two are controlled by the target.

Radar backscatter is dependent upon not only the surface and sub-surface geometry, but also upon the dielectric properties. The energy incident on the terrain surface is "specularly" or "diffusely" reflected in varying proportions depending upon the roughness of the terrain. Surface roughness is a geometric property of the terrain; it is not an absolute roughness, but rather roughness expressed relative to wavelength units. A smooth surface is characterized by specular or mirror-like reflection with the angle of incidence determining the orientation of the reradiation pattern (Figure 1A). If surface irregularities are a significant fraction of a wavelength, more energy will be scattered at angles other than near specular (Figure 1B). If radar wave penetration and volume scattering is involved, sub-surface geometry also governs the reradiation pattern. A change in both the shape and relative magnitude of the reradiation pattern can be induced by increasing the dielectric constant.

Lundien [1966, 1971] examined in the laboratory the effect of soil moisture on radar return, while MacDonald and Waite [1971] using commercially available imaging radars (K-band multipolarization) showed that differences in gross soil moisture content could be determined qualitatively. Measuring the microwave return under natural conditions and with quantitative soil moisture and configuration information was begun in August, 1972 at the University of Kansas Center for Research, Inc. Preliminary results of backscatter measurements [Ulaby, 1974] taken on two fields by a truck-mounted 4 - 8 GHz, FM-CW radar system (Table 1) indicated that radar response to soil moisture content is highly dependent upon the surface roughness, microwave frequency, and look angle. Ulaby et al. [1974] in a discussion concerning a new model based on the skin depth (attenuation) concept for soil moisture using the 4 - 8 GHz system, concluded that within 10° of nadir, a strong and essentially linear relation was observed at all frequencies between the scattering coefficient and the effective attenuation coefficient. They also noted that at

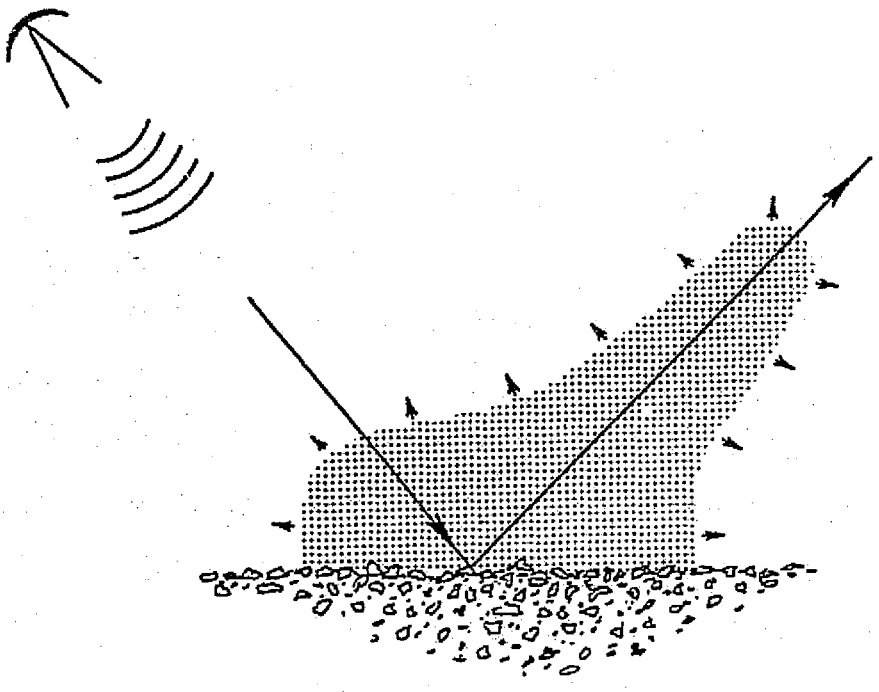

(A) Specular Reflection

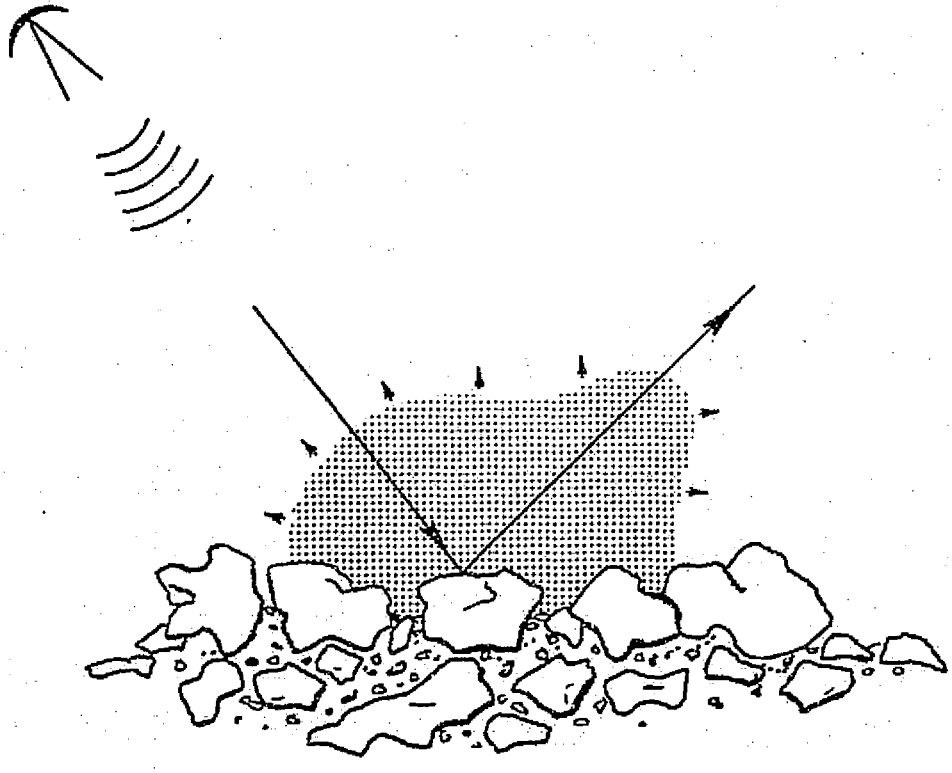

(B) Diffuse Reflection

Figure 1. Specular Versus Diffuse Reflection.

TABLE 1

Type:	FM-CW
Modulating Wave Form:	Triangular
Center Frequencies:	4.7 GHz, 5.9 GHz, 7.1 GHz
Bandwidth: ΔF	1.2 GHz
Transmitter Power:	5 watts
IF Frequency: F_{IF}	87 KHz
IF Bandwidth: ΔF_{IF}	5 KHz
Antennas:	
Height above ground	67 feet
Transmitting antenna diameter	2.5 feet
Receiving antenna diameter	3.0 feet
Feeds	ridged waveguide, dual polarized
Beamwidths of the patterns product $(G_T(\theta, \phi) \cdot G_R(\theta, \phi))$	Elevation: 4°-3.1° (over 4-8 GHz)
	Azimuth: 3.8°-2.9° (over 4-8 GHz)
Look Angle Range: θ	0° - 80° from the vertical.

larger angles the sensitivity to changes in the effective attenuation coefficient and therefore in moisture content, was greater at the lower frequency. The skin depth at the highest moisture values for the 7.1 GHz frequency is approximately one centimeter [Ulaby, et al., 1974] which meant:

1. These measurements are less valuable for determining moisture values to significant depths.

2. The validity of the "ground-truth" data is questionable due to the thin moisture region and the difficulty involved in defining a rough surface.

They concluded that lower frequencies and therefore greater skin depths appear necessary if the total moisture content for a given soil thickness is to be directly measured rather than inferred from the moisture in very thin surficial layers [Ulaby, et al., 1974]. Table 2 illustrates skin depth as a function of soil moisture and frequency.

The measurement of the complex dielectric constant affords an excellent estimate of the soil moisture content due to its dependency to the content of free water in the soil. Moreover, at the lower microwave frequencies, Lundien [1966] has shown that the effects of soil type on the value of the dielectric constants are overriden by the effects of the free water content in the soil. Cihlar and Ulaby [1974] have noted that the sole parameter affecting the frequency dependence of the dielectric properties of moist soil is water. For a smooth surface, the power reflection coefficient is directly related to this parameter. However, as the surface roughness increases this optimum relationship is no longer true and a correction factor must be applied. Experiments by Batlivala and Ulaby [1975] have resulted in a detailed analysis of the effect of roughness on σ^o for bare fields. Their objective was to determine an optimum set of radar parameters (frequency, polarization, incidence angle) such that the σ^o value of the ground is virtually independent of surface roughness but not at the expense of a reduction in sensitivity to soil moisture variations. The following discussion is a summary of their analysis.

Experimentation was carried out using a truck-mounted 2 GHz - 8 GHz, microwave active spectrometer (MAS) system [Oberg and Ulaby, 1974] on three fields of considerably different surface roughnesses, but each denuded of any vegetative cover. The roughness was calculated using rms height with respect to the mean surface of the ground. The smooth, moderate, and rough fields were found

TABLE 2 Skin Depth δ in cm for the Soil Moisture Profiles of Figure 5.

Profile				Incidence Angle							
Number[b]	Date of Measurement	Moisture Content[a]	Frequency in GHz	0°	10°	20°	30°	40°	50°	60°	70°
1	8/18/72	4.8	4.7	6.2	6.2	6.2	6.2	6.2	6.2	6.2	6.2
			5.9	5.8	5.8	5.8	5.8	5.8	5.7	5.7	5.7
			7.1	5.5	5.5	5.4	5.4	5.4	5.4	5.4	5.4
2	8/15/72	15.8	4.7	3.3	3.3	3.3	3.3	3.3	3.3	3.3	3.3
			5.9	3.1	3.1	3.1	3.1	3.0	3.0	3.0	3.0
			7.1	2.8	2.8	2.8	2.8	2.8	2.8	2.8	2.8
3	8/29/72	24.0	4.7	1.4	1.4	1.4	1.4	1.4	1.4	1.4	1.4
			5.9	1.2	1.2	1.1	1.1	1.1	1.1	1.1	1.1
			7.1	1.0	1.0	1.0	1.0	1.0	0.9	0.9	0.9
4	9/5/72	30.2	4.7	1.4	1.4	1.4	1.4	1.4	1.4	1.4	1.4
			5.9	0.9	0.9	0.9	0.9	0.9	0.8	0.8	0.8
			7.1	0.7	0.7	0.7	0.7	0.7	0.7	0.7	0.7
5	8/25/72	20.0	4.7	1.1	1.1	1.1	1.1	1.1	1.1	1.0	1.0
			5.9	0.9	0.9	0.9	0.9	0.8	0.8	0.8	0.8
			7.1	0.7	0.7	0.7	0.7	0.7	0.7	0.7	0.7
6	c	20.0	4.7	1.5	1.5	1.5	1.5	1.5	1.5	1.4	1.4
			5.9	1.2	1.2	1.2	1.2	1.2	1.2	1.2	1.1
			7.1	1.0	1.0	1.0	1.0	1.0	1.0	1.0	0.9

[a]Average moisture content of the top 5 cm of soil m_{we} in percent by weight.

[b]Moisture profiles are shown in Figure 5.

[c]Hypothetical case, moisture profile assumed constant with depth.

(After Ulaby, et al., 1974).

to have values of 0.88 cm, 2.6 cm and 4.3 cm respectively. The three fields were chosen such that they most closely represented typical plowed fields for the rough category, and plowed-then-disced for the moderately rough category. The smooth field is a somewhat rarely occuring category but elimination from consideration would have implied a bias toward rougher fields.

Each radar data set utilized 5 angles of incidence from 0° (nadir) through 40° in 10° intervals for both HH and VV polarizations at eight central frequencies between 2 GHz and 8 GHz (Table 3). It was necessary to use spacial and frequency averaging to reduce signal fading.

Soil samples were obtained at 8 different locations for each field per data set at five depths: 0-1 cm, 1-2cm, 2-5 cm, 5-9 cm, and 9-15 cm. Moisture contents were determined by the weight and by the bulk density methods.

Surface roughness, as previously discussed, is a geometric property of the terrain and is expressed relative to the wavelength. For a field of a given surface configuration, an increase in frequency would imply a rougher field in terms of the electromagnetic radiation impinging upon it. Figure 2 illustrates this point. It should be further noted that where the curves intersect, the effect of surface roughness is minimal; those values are 4° for 2.75 GHz, 10° for 5.25 GHz and 20° for 7.25 GHz.

When considering the effect of roughness on the spectral and the moisture responses of σ°, the following conclusions are apparent: at nadir (Figure 3A) σ° displays little variation between 5.25 and 7.25 GHz but exhibits a decreasing response with frequency between 2.25 and 5.25 GHz for moderate and rough fields. At 10°, σ° for the rough field decreases with frequency but at a slower rate than for the same bandwidth at nadir, the moderately rough field displays an independence to frequency and the smooth field reverses slope, while at 20° (Figure 3C), σ° for the smooth field increases rapidly. The σ° response to soil moisture is illustrated in Figure 4 (a,b)for three surface roughness profiles at 2.75 GHz for two angles of incidence; 0° (nadir) and 10°. Slope is an indicator of the σ° response to moisture and is referred to as sensitivity given in dB/.01 g/cm^3. For example, the sensitivity of the smooth field (Figure 4a) is the greatest at nadir while the sensitivity of the rough field is the least.

At 10° (Figure 4b) just the opposite observation holds. This would imply that the roughness effect can be minimized by operating at an angle between 0° and 10°.

TABLE 3. MAS 2-8 System Specifications

Type:	FM-CW
Modulating Waveform:	Triangular
Center Frequencies:	2.75, 3.25, 4.75, 5.25, 5.75, 6.25, 6.75, 7.25 GHz
FM Sweep: ΔF	450 MHz
Transmitter Power:	40 mW
IF Frequency: F_{IF}	50 KHz
IF Bandwidth: ΔF_{IF}	6 KHz
Antennas:	
Height above ground:	20 m
Transmitting antenna diameter:	91.5 cm
Receiving antenna diameter:	91.5 cm
Feeds:	Log periodic
Effective Two-way beamwidth:	5.4° at 2.75 GHz/ 2.2° at 7.25 GHz
Incidence angle range:	0° (nadir)-80°
Polarization:	Horizontal transmit-Horizontal receive (HH) Vertical transmit-Vertical receive (VV)
Calibration:	
Internal	Delay line
External	Luneberg lens

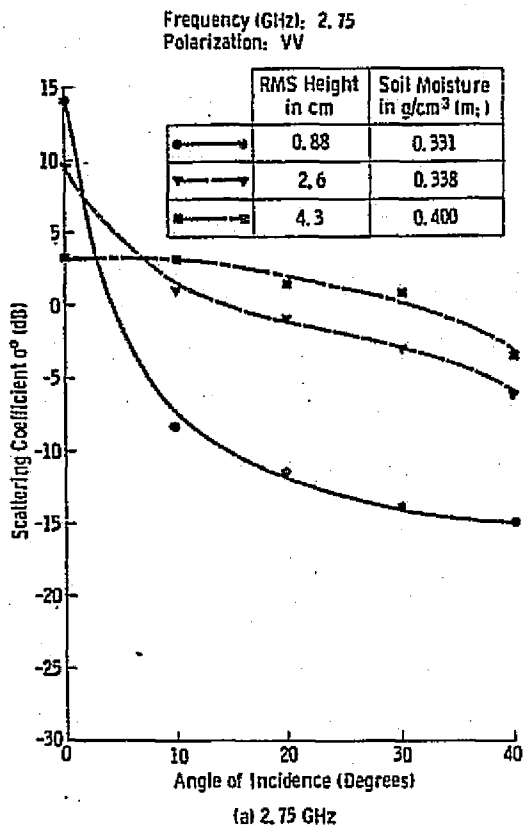

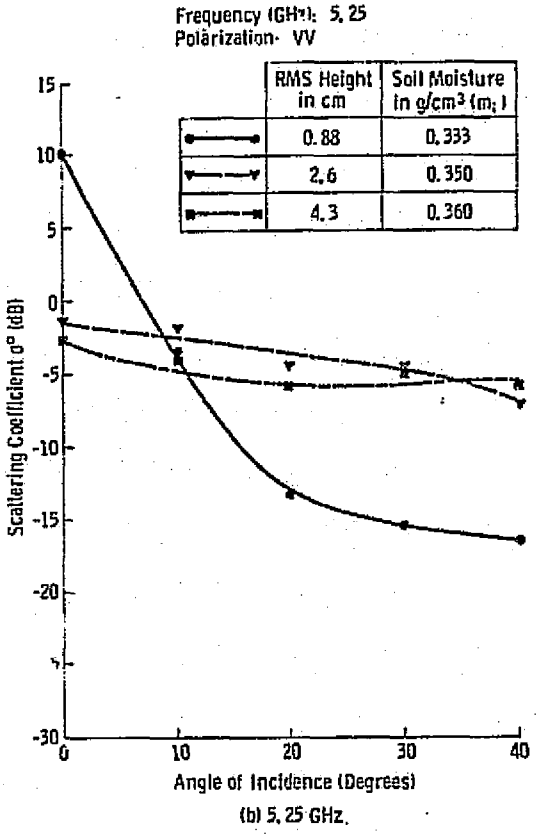

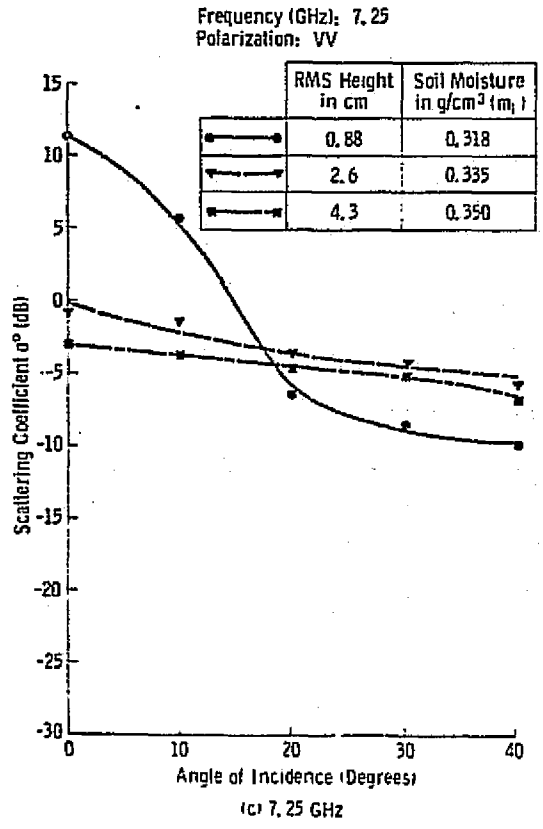

Figure 2. Angular response of the scattering coefficient for the smooth, medium rough, and rough fields for high levels of moisture content at (a) 2.75 GHz, (b) 5.25 GHz, and (c) 7.25 GHz. (From Batlivala and Ulaby, 1975).

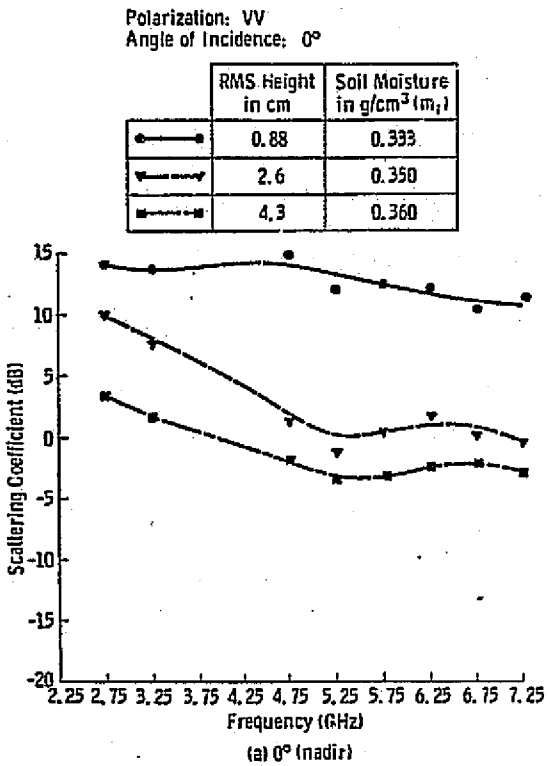

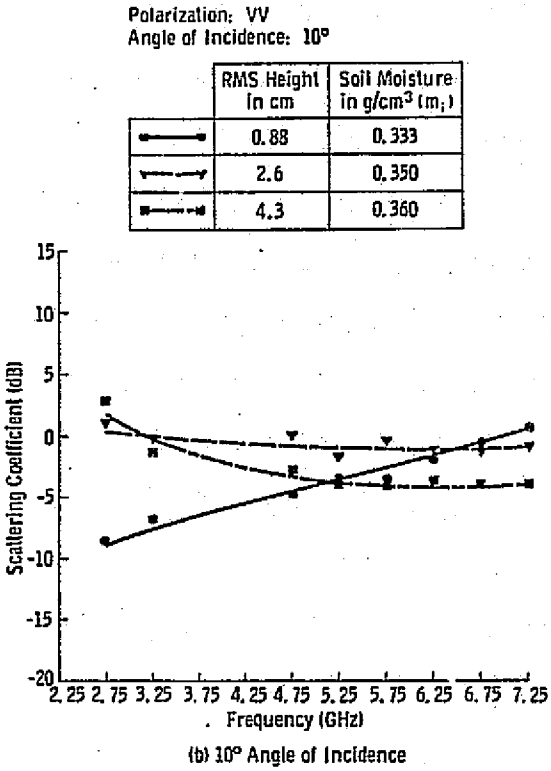

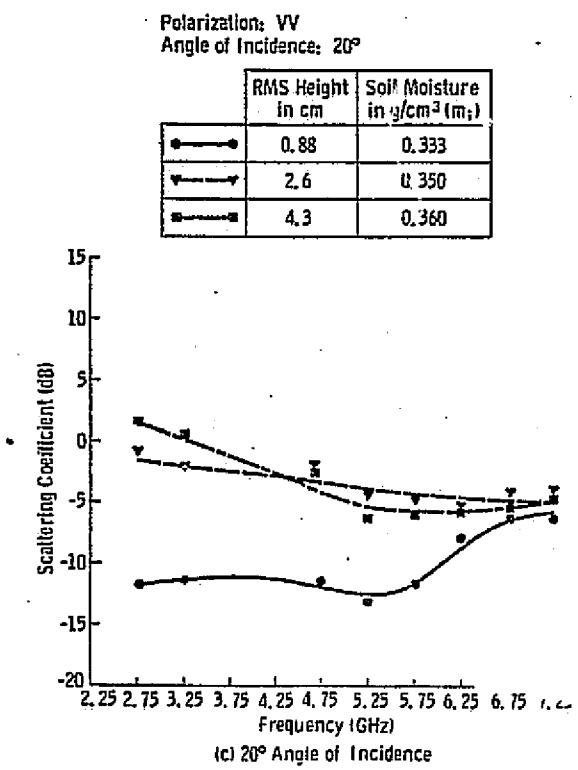

Figure 3. Spectral response of the scattering coefficient for smooth, medium rough, and rough fields for high level of moisture content at (a) 0° (nadir), (b) 10° and (c) 20° angle of incidence. (From Batlivala and Ulaby, 1975).

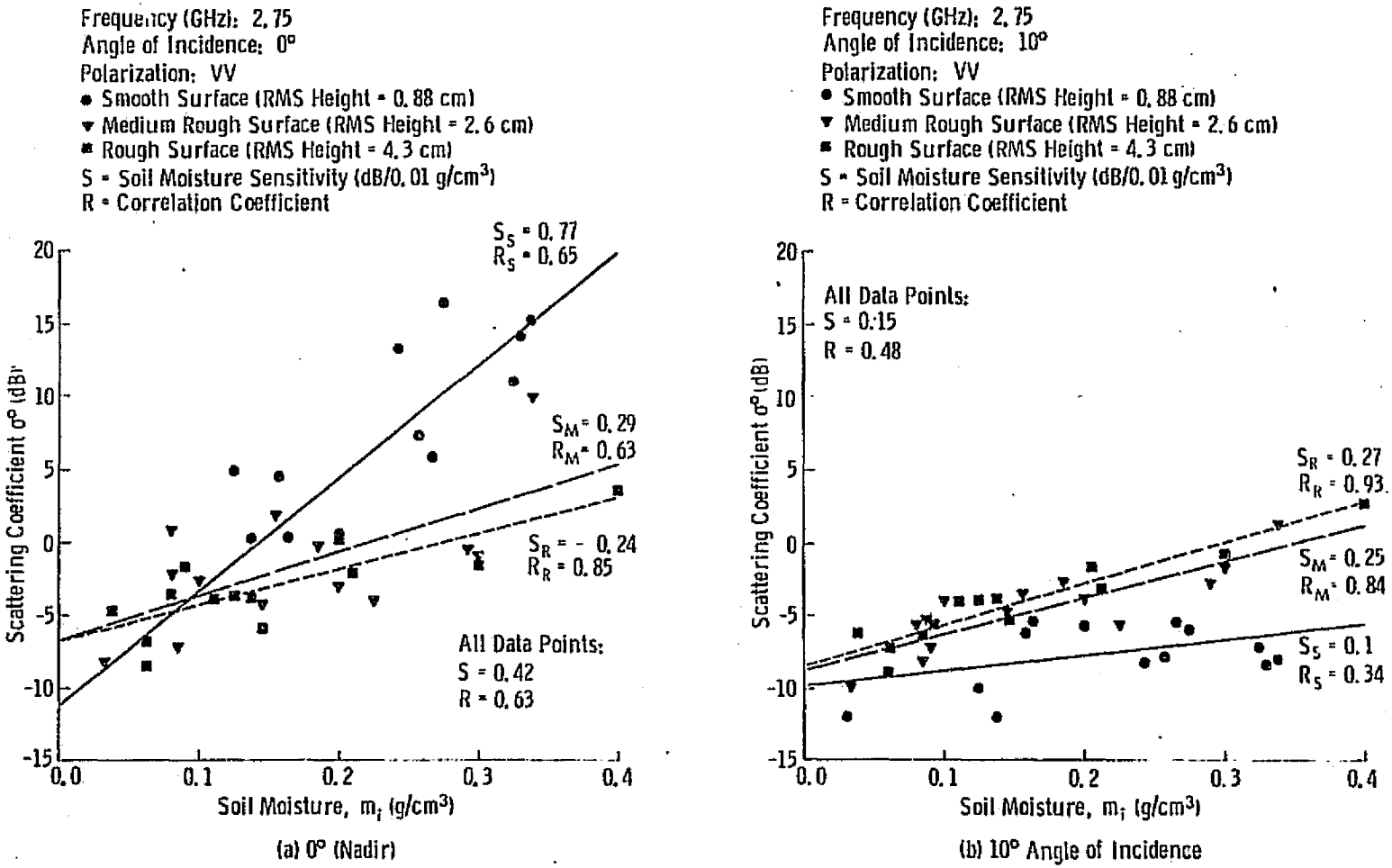

Figure 4. Soil moisture responses for the three surface roughness profiles at 2.75 GHz for (a) 0° (nadir) and (b) 10° angle of incidence. (From Batlivala and Ulaby, 1975).

The effect of surface roughness on the choice of optimum system parameters is seen in Figures 5 - 7 which depict calculated linear regression lines of σ^o as a function of soil moisture content. As the frequency is increased the radar response is more sensitive to roughness at all soil moisture conditions but a decrease in sensitivity occurs for the soil moisture. Thus, operating at 0^o (nadir) is undesirable due to this large change in σ^o with respect to rms height especially at 0.35 g/cm^3. (Note: 14 dB at 2.75 GHz, 18 dB at 4.75 GHz, and 16 dB at 7.25 GHz).

At an incidence angle of 10^o, the response to the variation in surface roughness (Figure 6) between σ^o for the smooth field and σ^o for the rough field decreases as the frequency is increased from 2.75 GHz to 7.25 GHz. The optimum condition is one where the moisture curves for σ^o are horizontal lines, parallel, and at maximum separation. The frequency which best satisfies these three conditions is 4.75 GHz.

Variations in σ^o at 20^o (Figure 7) also decrease as frequency increases, but the data indicates that for roughness to become an independent variable, a frequency greater than 7.25 GHz is necessary. Increasing frequency or angle results in a reduction in the magnitude of sensitivity, the latter represented in terms of separation between the curves. Thus it appears that the optimum frequency is 4.75 GHz, VV polarization at 10^o incidence angle.

To expand the number of available angles between 0^o and 20^o, a non-linear, interpolation technique was employed to evaluate the σ^o values at 3.3^o, 6.7^o, 13.3^o and 16.7^o. This procedure was applied for each data set at each frequency and polarization. Hence a new data base consists of 8 frequencies, 9 angles and two polarizations; a linear regression analysis was performed for each data set. Optimum correlation coefficient, sensitivity and frequency plotted as a function of incidence angle for moderately rough and rough fields are graphically illustrated in Figure 8. The optimum correlation is at the maximum (0.89) at 10^o and at 2.75 GHz, for both polarizations. The optimum frequency in the 0^o to 20^o angular range varies between 2.75 GHz and 3.25 GHz. When the data is combined for the moisture response for smooth, moderate, and rough fields (Figure 9), the optimum parameters exhibit a strong dependence on incidence angle.

These conclusions were based upon optimum sensitivity and correlation coefficient considerations; Figures 8 and 9 indicate an angular range of approximately 7^o to 15^o as optimum. An optimum frequency of about 3 GHz is suggested by Figure 8 while Figure 9 suggests a frequency of about 5 GHz; 4 GHz is recommend-

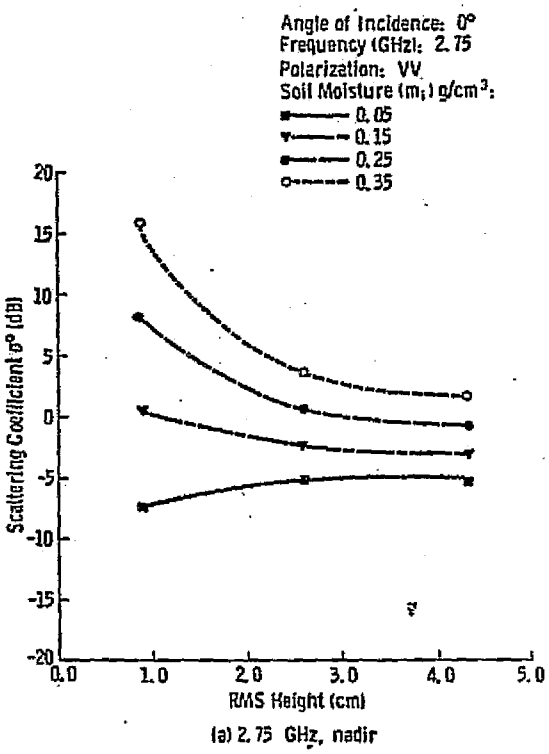

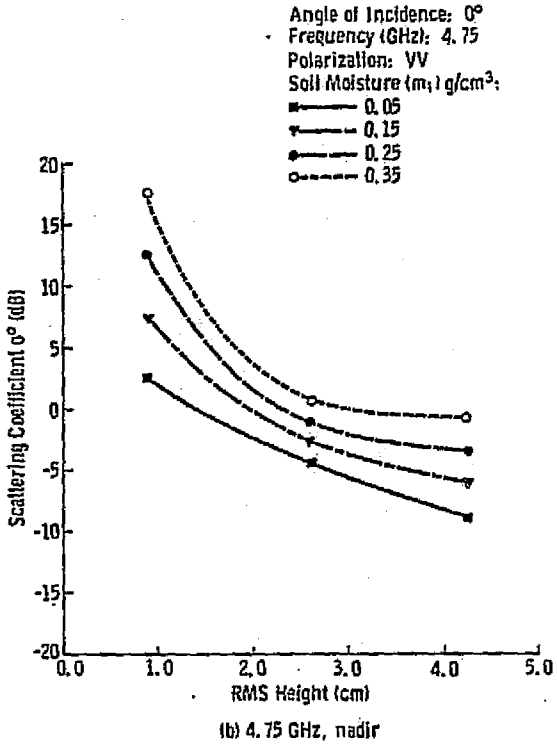

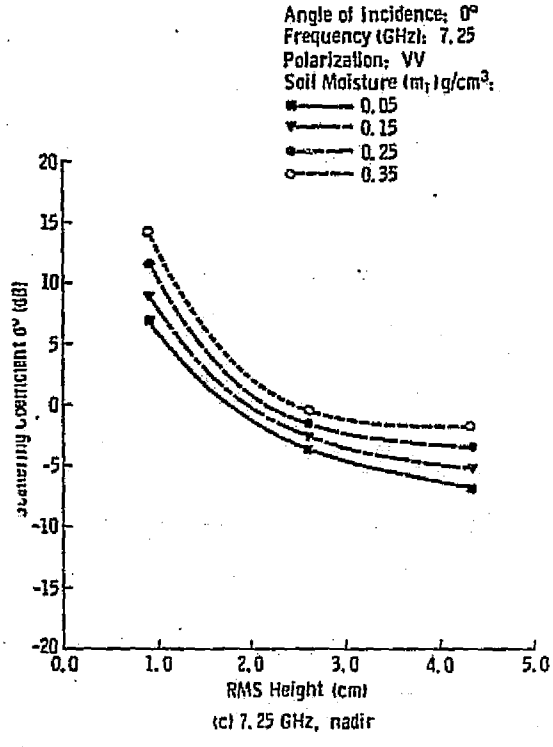

Figure 5. Scattering coefficient as a function of surface roughness at nadir for four moisture conditions at (a) 2.75 GHz, (b) 4.75 GHz, and (c) 7.25 GHz. (From Batlivala and Ulaby, 1975).

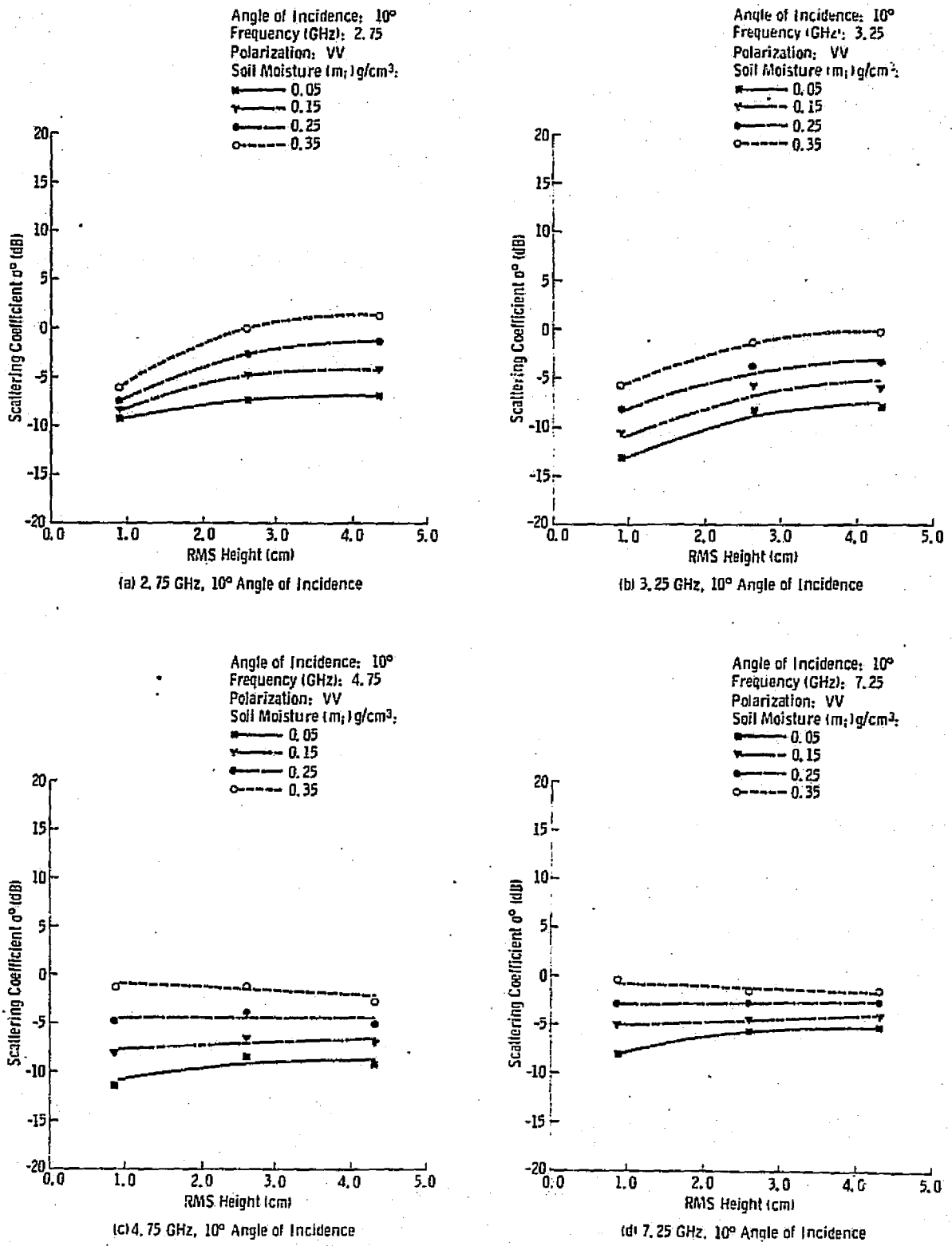

Figure 6. Scattering coefficient as a function of surface roughness at an angle of incidence of 10° for four moisture conditions at (a) 2.75 GHz, (b) 3.25 GHz, (c) 4.75 GHz, and (d) 7.25 GHz. (From Batlivala and Ulaby, 1975).

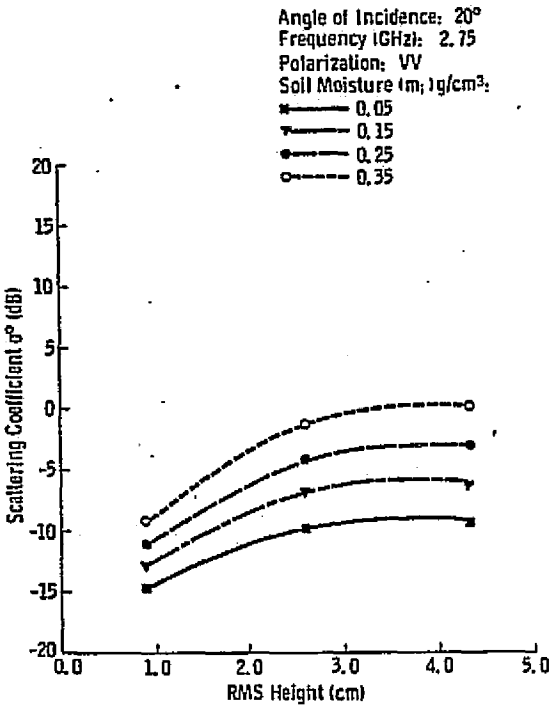

(a) 2.75 GHz, 20° Angle of Incidence

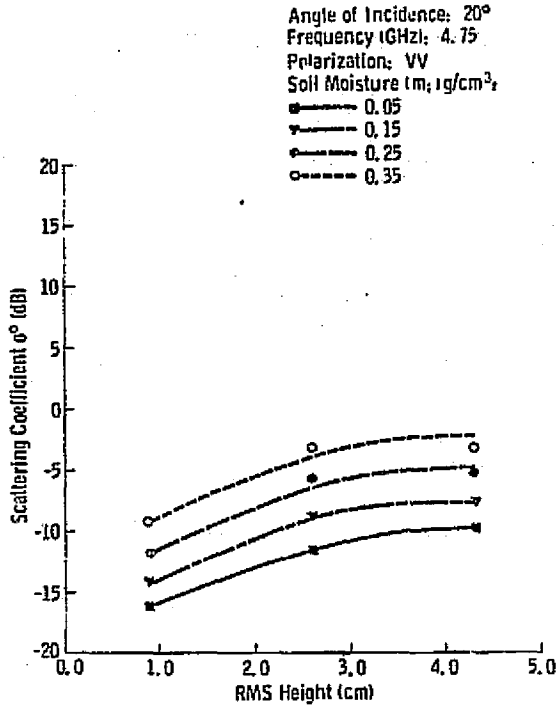

(b) 4.75 GHz, 20° Angle of Incidence

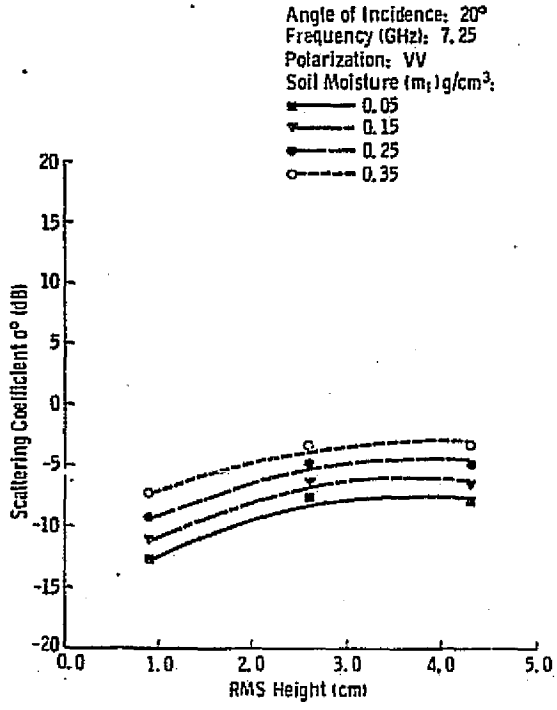

(c) 7.25 GHz, 20° Angle of Incidence

Figure 7. Scattering coefficient as a function of surface roughness at an angle of incidence of 20° for four moisture conditions at (a) 2.75 GHz, (b) 4.75 GHz, and (c) 7.25 GHz. (From Batlivala and Ulaby, 1975).

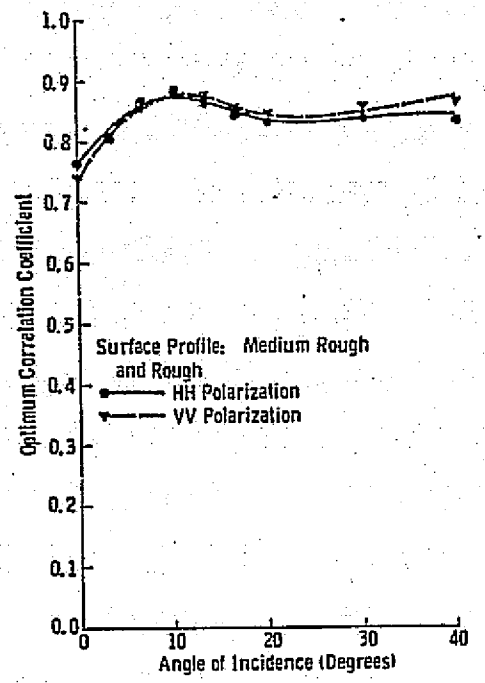

(a) Optimum Correlation Coefficient

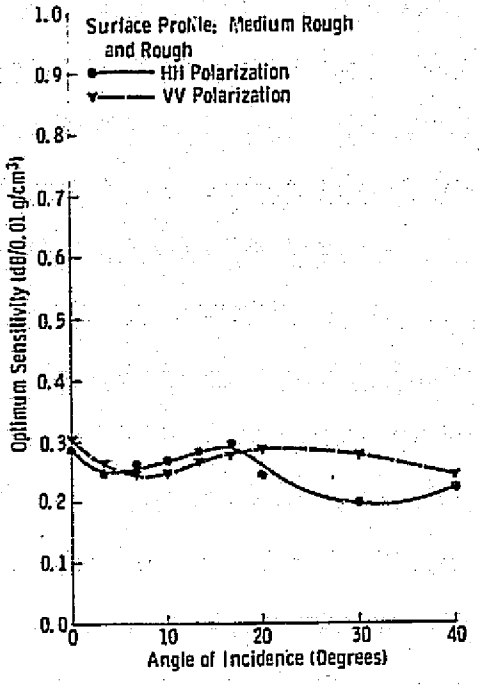

(b) Optimum Sensitivity

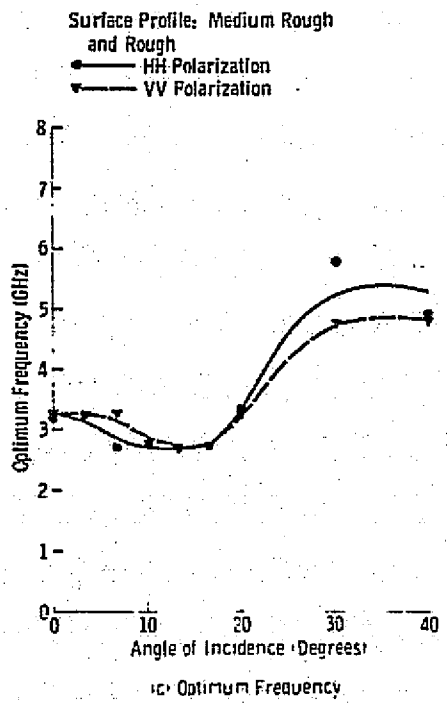

(c) Optimum Frequency

Figure 8. Optimum (a) correlation coefficient, (b) sensitivity, and (c) frequency plotted as a function of angle of incidence for the medium rough and rough surface profiles combined. (From Batlivala and Ulaby, 1975).

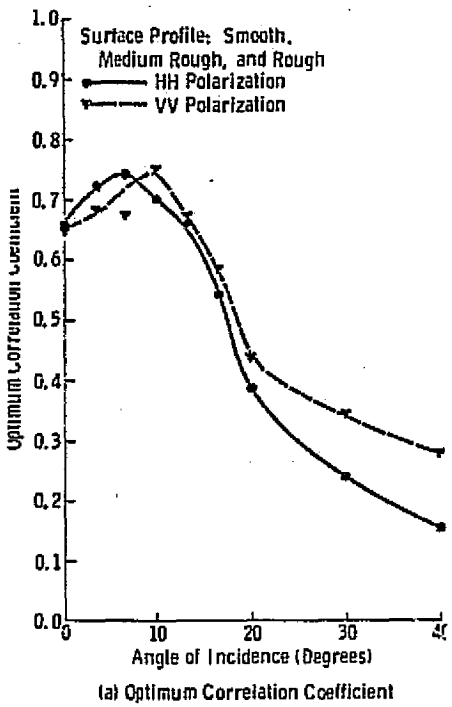

(a) Optimum Correlation Coefficient

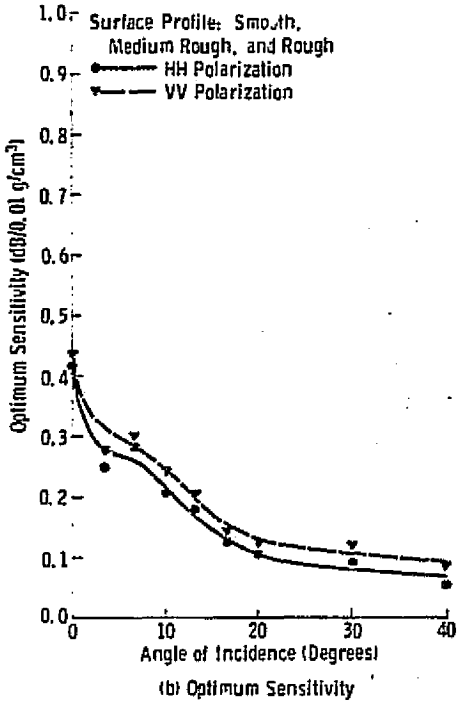

(b) Optimum Sensitivity

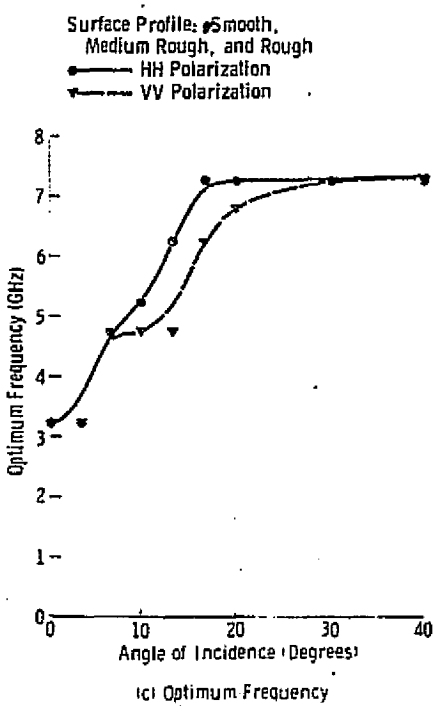

(c) Optimum Frequency

Figure 9. Optimum (a) correlation coefficient, (b) sensitivity, and (c) frequency plotted as a function of angle of incidence for the smooth, medium rough, and rough surface profiles combined. (From Batlivala and Ulaby, 1975).

ed as a compromise. Furthermore, both HH and VV polarizations displayed approximately the same moisture response.

The preceding discussion was covered in considerable detail because it represents the most recent work in the field of soil moisture detection utilizing radar in which ground data was an integral part of the analysis. Many of the following recommendations for monitoring soil moisture from space are the direct result of this investigation.

One further point should be noted: while the above results are applicable for fields void of any vegetative cover, similar observations have been obtained when considering vegetation [Ulaby, 1975; Ulaby et al., 1975]. The correlation coefficient between σ^o and soil moisture content is greatest at a 10^o angle of incidence at 4.7 GHz even though the presence of vegetated cover tends to reduce the sensitivity of σ^o to soil moisture variations.

3.0 CONCLUSIONS

A tool of great potential exists whereby soil moisture conditions could be monitored on a regional scale if the proper airborne platform were utilized. If the objective were to determine a temporal change in soil moisture through repetitive coverage of a given area, a revisit time of 1 to 30 days, the latter being a maximum, is required of any water resources satellite program (depending upon the area, parameters interested in, etc.) (periodicity of coverage obtained from tables of measurable parameters from a report entitled, "Satellite Data Collection User Requirements: Report of the NASA Ad Hoc Committee on Hydrology). A short revisit time is necessary due to the extreme changability of this surface phenomenon. To realize the maximum useage of data retrieved in improving hydrological forecasting and water resource management, an average revisit time of 4 days is suggested. This requirement leads to the necessity of using very large swath widths, about 400 km, to ensure full coverage of the continental United States plus Alaska. Based upon the optimum angular range of incidence angles (7^o - 15^o) for monitoring soil moisture conditions, an orbiting spacecraft at 1100 km would produce a ground swath width of about 160 km. It should be noted that design considerations dictate an image swath width based upon an angle of incidence range of 7^o to 22^o. While the overall dimensions of the swath approximates 300 km, any point beyond the optimum angle (beyond 15^o) would fall into the ambiguity

category. Exactly where the cutoff is for useable data beyond the 15° angular range is speculative. This problem can only be resolved when more data becomes available.

The above discussion centers on the criteria of repetitive coverage in order to insure accurate monitoring of soil moisture variations on a temporal basis. If on the other hand, the objective was to map soil moisture content from a single mission, the complications induced by the 4 day revisit requirement are eliminated. However, the optimum angular range of incidence angles necessary for maximum data retrieval remains the same. Moreover, image swath width is still a major consideration from the standpoint of mission planning since it may now be necessary to fly more than one pass for a given area to obtain complete coverage. Such a consideration would be unfeasible for same-day coverage if an orbital platform were utilized.

The proposed system resolution of 100 meters [Claassen, 1975] should provide sufficient information for both regional analyses and some local detail. Greater spacial resolution is impractical due to power requirements [McMillan, 1975]; poorer resolution would hamper data analyses for all but gross variations in soil moisture.

In conclusion, the following recommendations are submitted for application toward an operational system. The recommended radar parameters are:

optimum angle of incidence range:	7° - 15°
optimum frequency:	4 GHz
polarization:	HH or VV
resolution:	100 meters or better

A revisit time of 4 days is recommended.

BIBLIOGRAPHY

1. Batlivala, P. P. and F. T. Ulaby, 1975, Effects of roughness on the radar response to soil moisture of bare ground: University of Kansas Center for Research, Inc., Lawrence, Kansas, RSL Technical Report 264-5, 44p.

2. Cihlar, J. and F. T. Ulaby, 1974, Dielectric properties of soils as a function of moisture content: University of Kansas Center for Research, Inc., Lawrence, Kansas, RSL Technical Report 177-47, 61p.

3. Claassen, J. P., 1975, A short study of a scanning SAR for hydrological monitoring on a global basis: University of Kansas Center for Research, Inc., Lawrence, Kansas, RSL Technical Report 295-1.

4. Edgerton, A. T., 1968, Engineering applications of microwave radiometer: Proceedings 5th International Symposium on Remote Sensing of Environment, University of Michigan, Ann Arbor.

5. Gates, D. M., 1964, Characteristics of soil and vegetated surfaces to reflected and emitted radiation: Proceedings 3rd International Symposium on Remote Sensing of Environment, University of Michigan, Ann Arbor.

6. Jackson, R. D., 1973, Diurnal changes in soil water content during drying: Field Soil Water Regime, Soil Sci. Soc. Am., vol. 39, p. 37-55.

7. Jean, B. R., C. L. Kroll, J. A. Richerson, J. W. Rouse, Jr., T. G. Sibley, and M. I. Wiebe, 1972, Microwave radiometer measurements of soil moisture: Technical Report TSC-32, Remote Sensing Center, Texas A & M University, College Station, Texas, 41p.

8. Luder, D. R., 1959, Gray Tones: in Aerial Photographic Interpretation, McGraw-Hill Book Co., New York p. 76-101.

9. Lundien, J. R., 1966, Terrain analysis by electromagnetic means, report 2, radar responses to laboratory prepared soil samples: U. S. Army Engineer Waterways Experiment Station Technical Report 3-693, Vicksburg, Mississippi.

10. Lundien, J. R., 1971, Terrain analysis by electromagnetic means: Technical Report No 3-693, Report 5, U. S. Army Engineer Waterways Experiment Station, Vicksburg, Mississippi.

11. MacDonald, H. C. and W. P. Waite, 1971, Soil moisture detection with imaging radars: Water Resources Research, vol. 7, no. 1.

12. McMillan, S., 1975, Synthetic aperture radar and digital processing: University of Kansas Center for Research, Inc., RSL Technical Memorandum 295-3, Lawrence, Kansas.

13. Oberg, J. M. and F. T. Ulaby, 1974, MAS 2-8 radar and digital control unit: RSL Technical Report 177-37, University of Kansas Center for Research, Inc., Lawrence, Kansas.

14. Poe, G. A., 1971, Remote sensing of the near-surface moisture profile of specular soils with multi-frequency microwave radiometry: Proceedings SPIE, vol. 27; also Final Technical Report 1684-1, Aerojet Gen. Corp., El Monte, Calif.

15. Reeves, C. C., 1973, Dynamics of playa lakes in the Texas high plains: Third Earth's Res. Tech. Satellite-1 Symposium, vol. 1, sec. 4, no. W13, p. 809-818.

16. Schmugge, T., P. Gloersen and T. Wilheit, 1972, Remote sensing of soil moisture with microwave radiometers: Goddard Space Flight Center, NASA, Greenbelt, Maryland, Preprint X-652-72-305, 32p.

17. Sui, Lin Lee, 1974, Dual frequency microwave radiometer measurements of soil moisture for bare and vegetated rough surfaces: Technical Report RSC-56, Remote Sensing Center, Texas A & M University, College Station, Texas.

18. Sobti, A., 1975, Terrain response to an orbiting microwave radiometer/scatterometer: (Ph. D. Thesis), University of Kansas Center for Research, Inc., RSL Technical Report 243-10, Lawrence, Kansas, 677p.

19. Stockhoff, E. H. and R. T. Frost, 1971, Polarization of light scattered from moist soils: Proceedings 7th International Symposium on Remote Sensing of Environment, University of Michigan, Ann Arbor.

20. Ulaby, F. T., 1973, 4-8 GHz microwave active and passive spectrometer (MAPS): CRES Technical Report 177-34, University of Kansas Center for Research, Inc., Lawrence, Kansas.

21. Ulaby, F. T., 1974, Radar measurement of soil moisture content: IEEE Trans. Antennas and Propagation, vol. AP-22, no. 2, p. 257-265.

22. Ulaby, F. T., 1975, Radar response to vegetation: IEEE Trans. Antennas and Propagation, Vol. AP-23, no. 1, p. 36-45.

23. Ulaby, F. T., T. F. Bush and P. P. Batlivala, 1975, Radar response to vegetation II -- 8 - 18 GHz band: IEEE Trans. on Antennas and Propagation, vol. AP-23, no. 5, p. 608-618.

24. Ulaby, F. T., J. Cihlar and R. K. Moore, 1974, Active microwave measurement of soil water content: Remote Sensing of Environment, vol. 3, p. 185-203.

25. Werner, H. D., et al., 1971, Application of remote sensing techniques to monitoring soil moisture: Proceedings 7th International Symposium on Remote Sensing of Environment, University of Michigan, Ann Arbor.

APPENDIX B

RSL TECHNICAL REPORT 295-3

VOLUME III

THE UNIVERSITY OF KANSAS SPACE TECHNOLOGY CENTER
Raymond Nichols Hall
2291 Irving Hill Drive—Campus West Lawrence, Kansas 66045

Telephone:

RADAR MEASUREMENT OF SNOW -- STATE OF THE ART

Remote Sensing Laboratory
RSL Technical Memorandum 295-11

Bradford C. Hanson

July, 1976

Supported by:

NATIONAL AERONAUTICS AND SPACE ADMINISTRATION
Goddard Space Flight Center
Greenbelt, Maryland 20771

CONTRACT NAS 5-22384

ABSTRACT

Improved snowpack melt forecasts are necessary to ensure the successful management of any water resource program where the major source of water is derived from snow melt runoff. Current technology has provided techniques whereby snowpack monitoring is feasible from spaceborne, remote sensing systems. ERTS has yielded improved methods for snowpack, data acquisition. Similar results have been obtained utilizing the NOAA-VHRR and the ESSA-9 systems. However, problems of resolution, cloud cover restrictions, canopy problems, and non-continuous snow cover ambiguities have often rendered the images less useful than originally expected.

Experiments with active microwave sensing systems have been performed; the University of Kansas 1-8 GHz Microwave Active Spectrometer (MAS 1-8) system was used to measure the backscatter response of snow covered ground between 21 February and 23 April 1975. Simultaneous ground truth data consisted of soil moisture, soil temperature profile, snow depth, snow temperature profile, and snow water equivalent. The preliminary results of the experiment indicate that the key parameter effecting the radar return is snow wetness when density stratification is not present within the snowpack under investigation.

RADAR MEASUREMENT OF SNOW -- STATE OF THE ART

Bradford C. Hanson

Snowpack water resources are of considerable importance in the management of irrigation systems, flood warning systems, hydroelectric-power schedules, and municipal and regional water supplies. Snowpack melt often provides the major source of water for power and human consumption for many areas throughout the world. In California for example, the Sierra Nevada snowpack accounts for more than 1/2 the total water supply and about 1/3 of the electric energy. Monitoring the seasonal snowpack parameters of surface temperature, total thickness, water equivalent, liquid water content, plus their continuous changes with respect to each other is necessary to ensure the successful management of any snowpack, water resource program.

An accurate water supply forecast depends upon an adequate and timely input of all necessary variables. The present technique employed for snowpack data acquisition is snow surveys. This traditional method consists of establishing a number of sample points within a given watershed for which physical sampling is performed. These measurements are then related to runoff by one of several methods, the historical normal, an index method, a water balance method, or by hydrologic methods. This information from aggregate spot locations has been and continues to be the basic snowpack evaluation technique for synthesizing the snow cover and resultant runoff for an entire watershed. However, too few data points are normally available to make reliable estimates of the snow cover and its physical condition. Adding additional ground stations is a costly venture. In mountainous regions of the U.S. for example, millions of dollars are spent each year at fixed locations to measure the snowpack. Moreover, improved forecasts are estimated to be worth 10^7 to 10^8 dollars per year to water users in the western United States alone (Useful Application of Earth-Oriented Satellites, 1969). Another problem is the timely input of data at regular intervals plus the necessity of data upon demand. Watershed areas in the mountainous regions of Arizona often undergo rapid change within a time span of a few days to a few hours.

Thus one must not only monitor vast areas incorporating an infinite number of sample points, but must also monitor on a periodic basis. The problems encountered from such a technique are numerous, but until recently, other methods were impossible due to the lack of the necessary technological advances.

Current technology has introduced the feasibility of airborne and spaceborne remote sensing systems for monitoring the snowpack. Watershed snowpack and streamflow data obtained and transmitted by ERTS have been used by Warskow et al., (1975) in operational and water management decisions for the Salt River project. However the satellite image gave only 14% reliability and was therefore used only to provide an overview for establishing snow course sites. Other problems have been encountered when applying ERTS data to snowpack prediction techniques; cloud cover is usually the rule rather than the exception especially immediately preceding and following a major snow storm. Bare rock often appears as snow cover (Washichek and Mikesell, 1975), canopy problems (Limpert, 1975; Kathibah, 1975), and imagery density and contrast variations which are not due to ground data (Aul and Ffolliott, 1975) are also encountered. Moreover at optical wavelengths, information retrieved is only from the surface of the snowpack; its physical condition at depth can only be inferred.

The National Environmental Satellite Service (NESS) began producing river basin snow maps on an experimental basis in the spring of 1973. The primary source of data was from the VHRR (Very High Resolution Radiometer) aboard the NOAA polar-orbiting satellites at 0.55 to 0.75 μm to 10.5 to 12.5 μm. Fog, cloud cover, and severe resolution restrictions rendered the data less useful than originally expected (Schneider, 1975). The U.S. weather service in Alaska employed NOAA-VHRR enhanced IR satellite imagery as an aid in the acquisition of daily synoptic snowmelt information for use with river forecasts (Seifert, et al., 1975). Again the major problems were cloud cover and image resolution, the latter being one mile which made variations within the snow cover impossible to detect. Resolution for the ESSA-9 system has been reported to be 4 kilometers (Rango, personal communication). Other difficulties encountered include the ambiguity between snow and clouds, identifying snow in areas of mountain shadows, and mapping snow where the snowcover is not continuous

(Barnes and Smallwood, 1975).

Edgerton et al., (1971) recorded microwave measurements of snow at 1.43, 4.99, 13.4 and 37 GHz and reported a direct relationship between brightness temperature and the water equivalent of dry snow (Figure 1). A general decrease in brightness temperature as total snowmass increased was also noted. This trend was confirmed in a later experiment in which the water equivalent was found to be the main factor influencing the brightness temperature from snow.

Cosgriff et al., (1960) completed one of the original measurements of snow cover with a truck mounted CW-Doppler scatterometer operating at X-band and K-band frequencies. Their results indicated that in general, snow had the effect of covering the backscatter from the terrain (Figure 2). Later Moore (1972) plotted this same data versus water content and illustrated a linear relationship between the normalized scattering coefficient and total water content (Figure 3). These data however, were at various temperatures and had insufficient ground truth to determine whether the results were actually due to the free water content within the snowpack or due to the underlying soil moisture. Vickers and Rose (1972) utilized a 2.7 GHz short pulse radar to investigate snowpack stratification. Their method has the drawback of needing ground based calibration for either the snow density or snow depth for the other variable to be remotely determined. Linlor (1974) measured the microwave reflection from various snow depths and found considerable variation with depth (Figure 4) but made no attempt to analyze the response. Waite and MacDonald (1970) observed differences in signal return between fresh snow and older perennial snow. They noted that in the past measured differences had been primarily attributed to moisture content variations within the snow pack, but in view of their data, they felt that these differences were probably due to volume scattering from inhomogeneities within the perennial snow. Moreover, cross polarization (HV) tended to bring out this effect more than like polarization (HH). Unfortunately, ground data did not exist for further confirmation of their results. The lack of simultaneous ground data in conjunction with aerial measurements over the snow pack is the major problem with most of the snow cover experiments to date. One notable exception is data acquired during the winter of 1974 and 1975 at The University of Kansas.

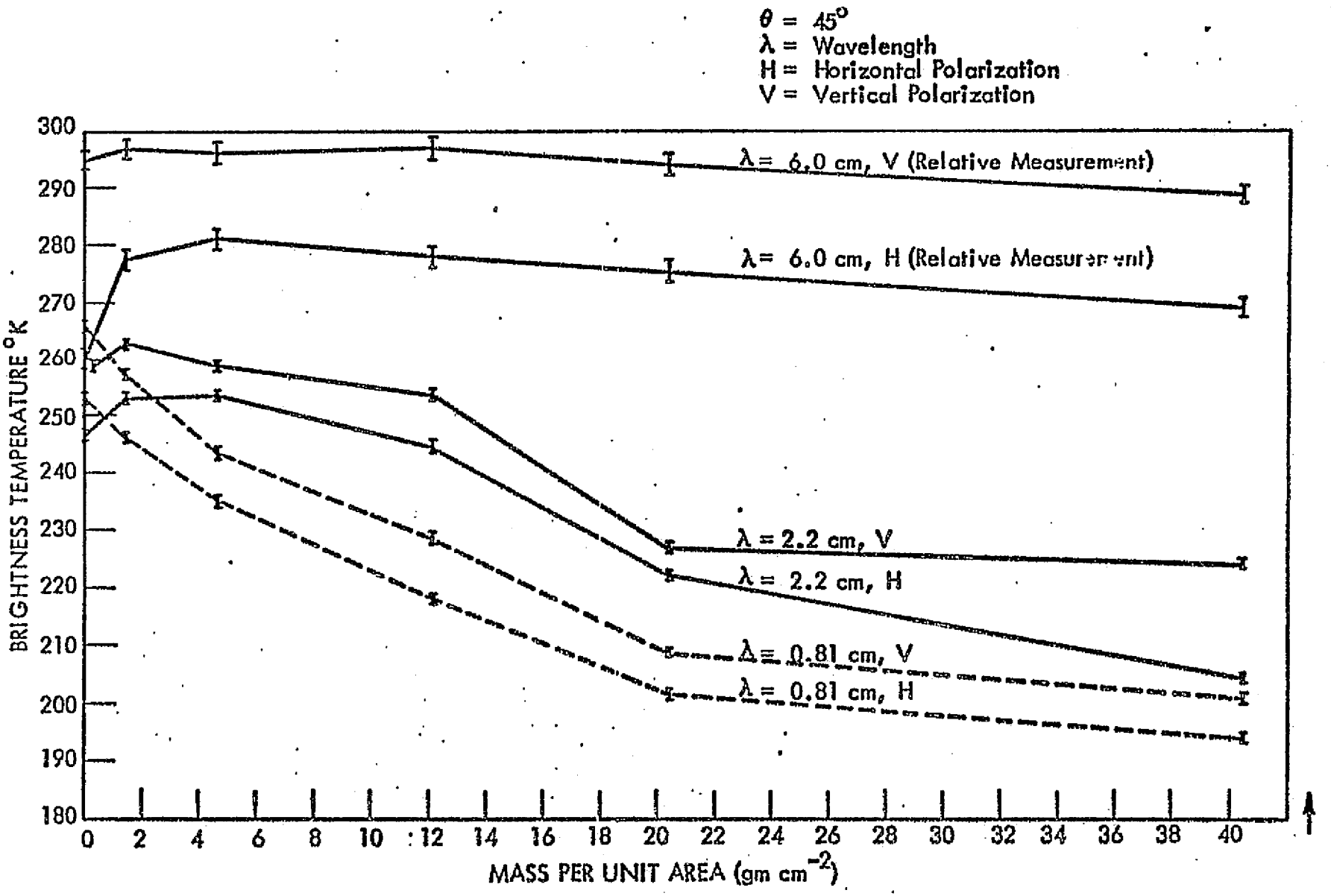

Figure 1. Brightness Temperature Versus Water Equivalent Dry Snow, Crater Lake, Oregon, 22 March 1970 (Edgerton, et al., 1971).

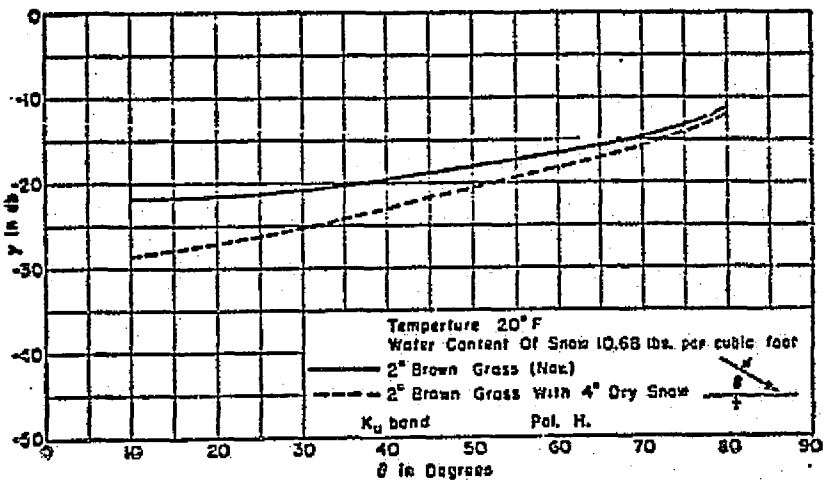

Figure 2. Effects of Snow on Gamma at Ku-Band. (Cosgriff, et al., 1960).

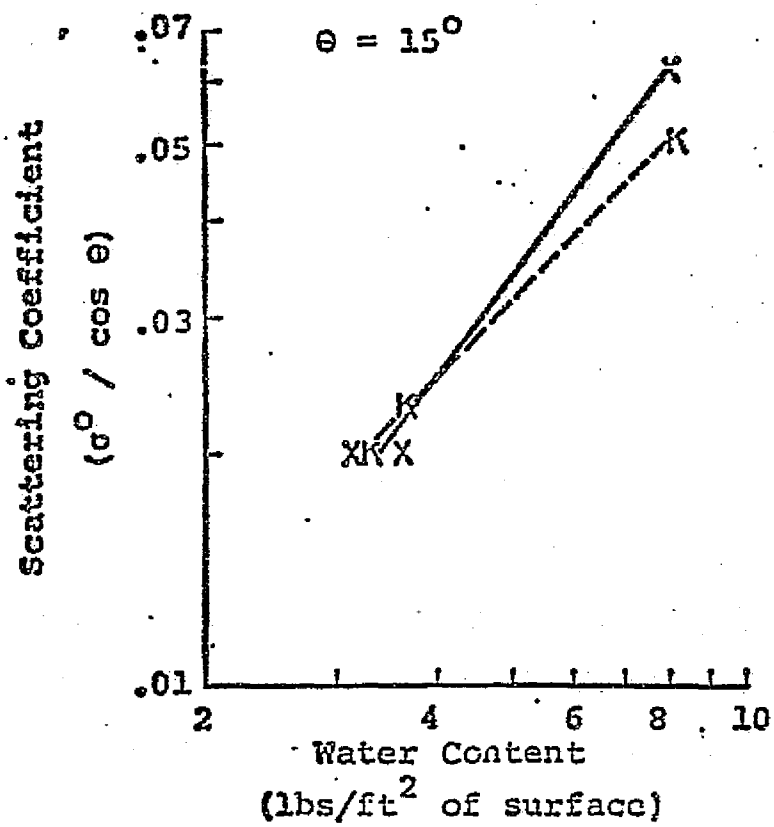

Figure 3. Variation of Backscatter with Snow Water Equivalent (Moore, 1972).

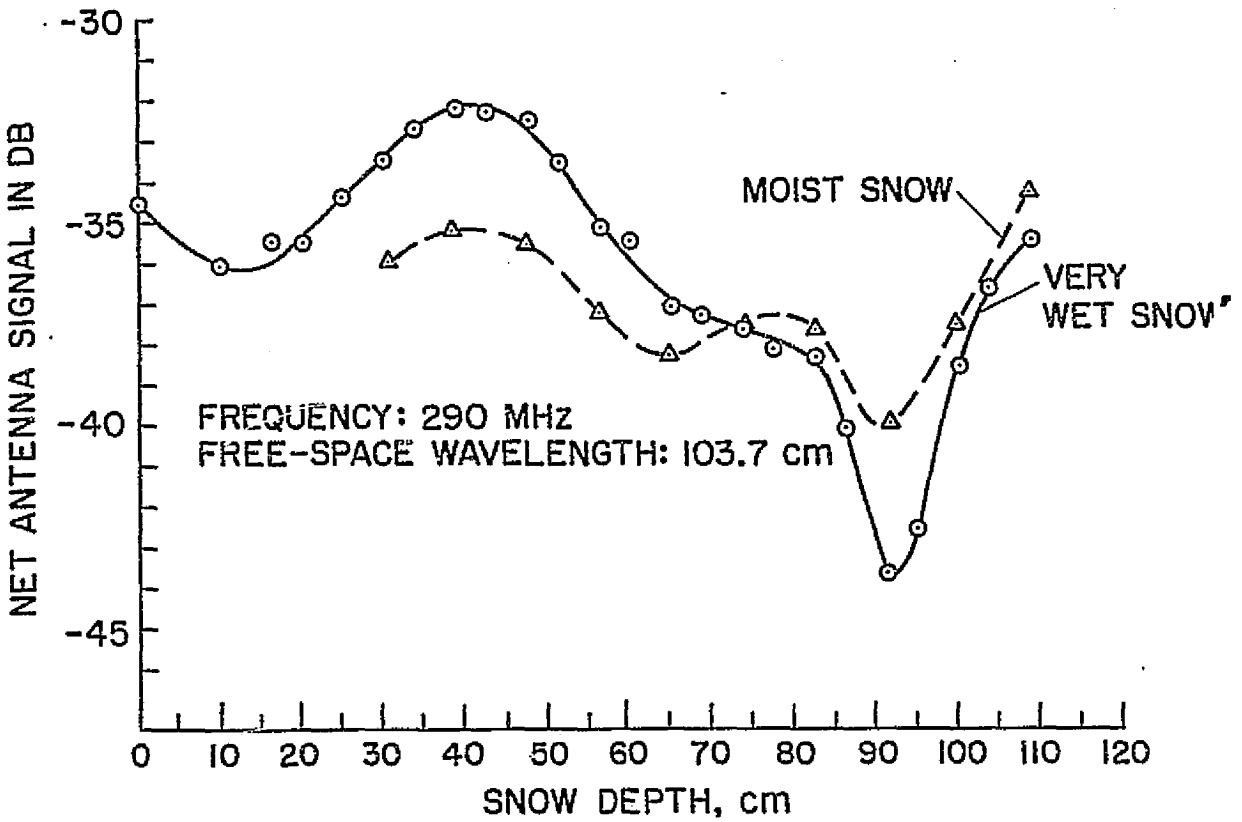

Figure 4. System Response vs. Snow Depth
(after Linlor, 1974).

Radar backscatter data were acquired with a truck-mounted 1-8 GHz Microwave Active Spectrometer (MAS 1-8) at eight frequencies within the 1-8 GHz range, for three polarizations (HH, HV, VV), and for incidence angles between 0° and 70°. Table 1 summarizes the system specifications.

Ground data (Hanson, 1975) was acquired in conjunction with the spectrometer measurements. Data collected consisted of soil moisture, soil temperature, air temperature, snow depth, snow temperature, and the stratigraphic profile within the snow pack. Since the experiment was conducted during the winter dormancy period, the height and physical condition of the ground cover was essentially constant.

Figures 5 and 6 illustrate scattering cross section, spectral responses for three distinct ground conditions. The maximum accumulation of dry snow encountered during the experiment was 15 cm; the effect of this minimal snow depth is demonstrated by Figure 5 which compares the σ° response for Run 4 (no snow) and Run 6 (snow cover - 15 cm dry powder). This is consistant with preliminary results obtained by Stiles and others (1976) (Table 2) which indicate that only a small effect should be observed for dry snow at depths of 15 cm or less since the skin depth for snow is greater than the overall snow depth.

Immediately before Run 8, a fine sleet intermixed with a light mist accumulated on the surface of the snow. Although snow wetness could not be measured, the surface was damp. Figure 6 illustrates the σ° response to the control set, Run 4, and the wet snow cover set, Run 8. The skin depth of "wet" snow at 1.0 GHz is 78 cm (Linlor, 1972; Table 2). Thus at 1.2 GHz, the 12 cm of wet snow (Run 8) in Figure 6 acts primarily as an attenuator of the backscatter from the underlying wet soil (Stiles et al., 1976). The skin depth for the wet snow cover at 7.25 GHz is comparable to or smaller than the 12 cm depth (Table 2) and therefore it is doubtful that there is any significant contribution to the 7.25 GHz response of Run 8 due to the underlying soil (Stiles et al., 1976).

The major conclusion derived from this experiment is that the key parameter effecting the radar return is snow wetness (Stiles et al., 1976). However it should be noted that snow depths were minimal and that climatic variations were such that density changes within the snow cover were not observed. In areas where greater snow depths occur for longer periods of

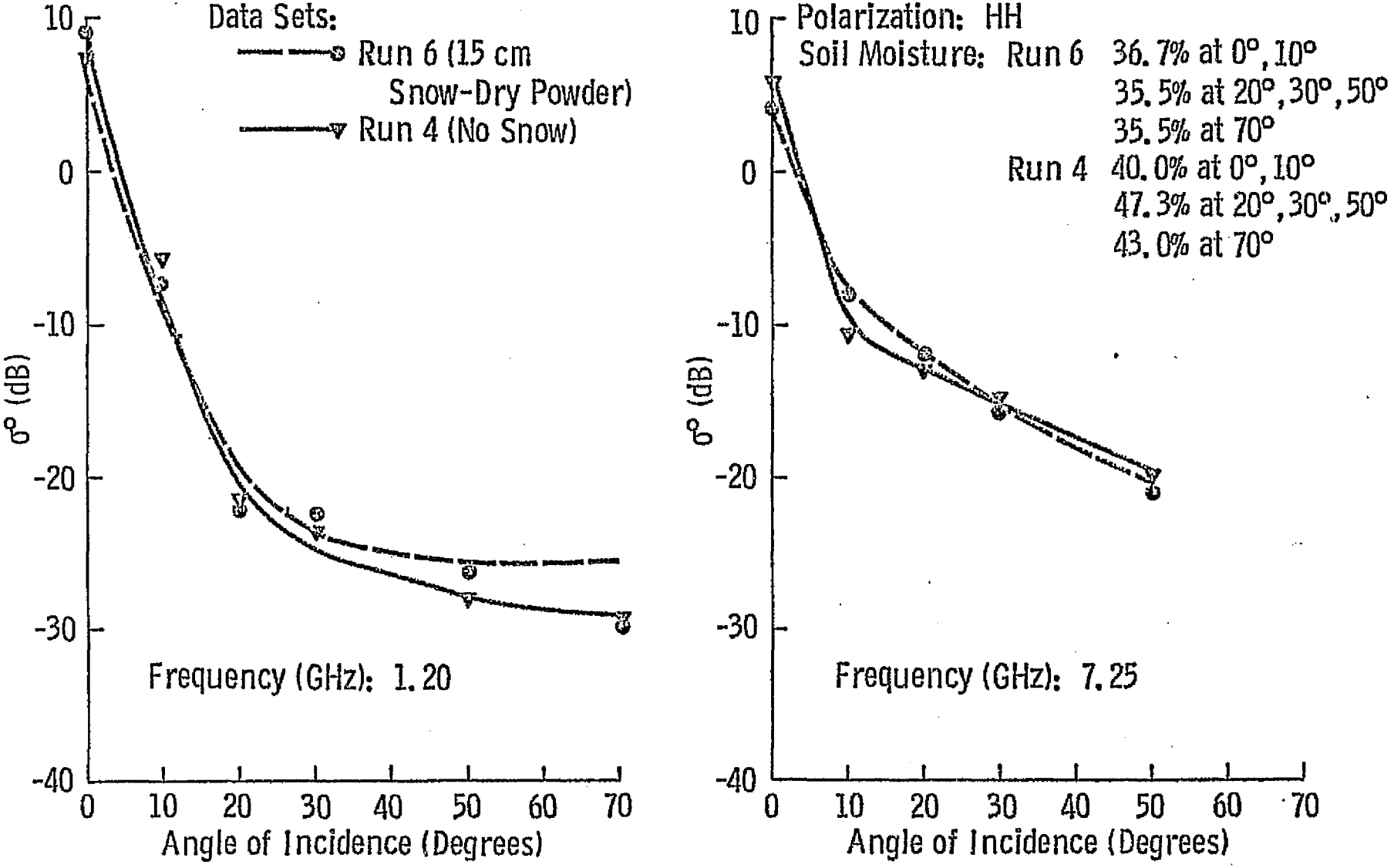

Figure 5. Angular Response of σ^{o} of Short Grass and Short Grass with a 15 cm Dry Powder Snow Cover. (From Stiles et al., 1976).

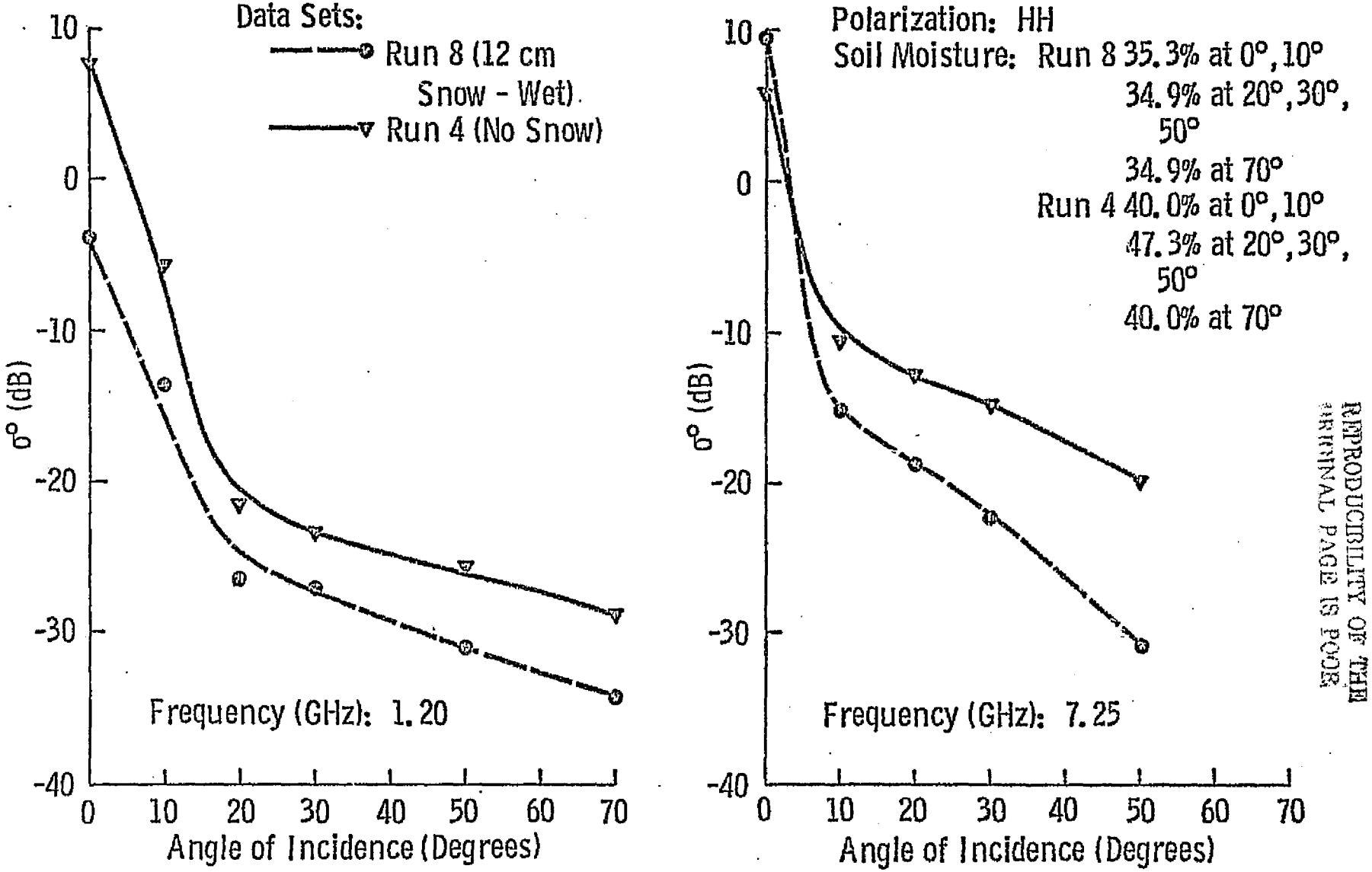

Figure 6. Angular Response of σ° of Short Grass and Short Grass with a 12 cm Wet Snow Cover. (From Stiles et al., 1976).

Table 1. MAS 1-8 Specifications

Type:	FM-CW
Modulating Waveform:	Triangular
Center frequencies:	1.2, 1.6, 2.25, 3.25, 4.25, 5.25, 6.25, 7.25 GHz
FM sweep: ΔF	400 MHz
Transmit power:	100 mW
IF: F_{IF}	49.5 KHz
IF bandwidth: ΔF_{IF}	11.5 KHz
Antennas:	
Height above ground:	19 m
Transmit antenna diameter:	1.22 m
Receive antenna diameter:	1.22 m
Feeds:	Dual polarized switchable 1-12 GHz log periodics
Effective system beamwidth:	12° at 1.2 GHz to 2° at 7.25 GHz
Incidence angle range:	0° (nadir) - 80°
Polarization:	Horizontal transmit-horizontal receive (HH) Horizontal transmit-vertical receive (HV) Vertical transmit-vertical receive (VV)
Calibration:	
Internal	Coaxial delay line
External	Luneberg lens

Table 2. Skin Depths for Snow

Description	Frequency (GHz)	K'	K''	tan δ	Skin Depth	Source
Dry Snow	37	1.9	.05	---	7 cm	Edgerton
Dry Snow	13.6	2.76	.03	---	38.8 cm	Edgerton
Wet Snow	1.0	1.5	---	10^{-1}	78 cm	Linlor
Wet Snow	8.0	1.5	---	10^{-1}	9.7 cm	Linlor
Dry Snow	1.0	1.32	.0002	---	548 m	Evans
Dry Snow	8.0	1.32	.0002	---	68 m	Evans
Foam 8.5% H_2O	1.83	---	---	---	43 cm	Linlor
Foam 8.5% H_2O	8.0	---	---	---	3 cm	Linlor
Saturated Snow	10	---	---	---	.9 cm	Linlor
Freshly Fallen Snow	3	1.2	---	.00029	100 m	Vickers
Freshly Fallen Snow	10	1.26	---	.00042	20.2 m	Vickers
Hard Packed Snow	3	1.50	---	.0009	28.9 m	Vickers
Ice	3	3.2	---	.0009	19.8 m	Vickers

(After Stiles et al., 1976).

time and stratification is evident, the key parameter effecting radar return may no longer be snow wetness.

In conclusion, the technology exists whereby orbital platforms containing accurate sensor packages are feasible for measuring snow pack conditions. The major stumbling block at the present time is the lack of specific information regarding the proper system design such that optimum data retrieval can be realized. This much-needed information can only be obtained after further experiments.

REFERENCES

1. Aul, J. S. and P. F. Ffolliott, 1975, Use of areal snow cover measurements from ERTS-1 imagery in snowmelt-runoff relationships in Arizona: Operational Applications of Satellite Snowcover Observations, NASA SP-391, p. 103-112.

2. Barnes, James C. and Michael D. Smallwood, 1975, Synopsis of current satellite snow mapping techniques, with emphasis on the application of near-infrared data: Operational Applications of Satellite Snowcover Observations, NASA SP-391, p. 199-214.

3. Cosgriff, R. L., W. H. Peake and R. C. Taylor, 1960, Terrain Scattering properties for sensor system design (Terrain Handbook II)," Ohio State University Experiment Station.

4. Edgerton, A. T., A. Stogryn and G. Poe, 1971, Microwave radiometric investigations of snowpacks: Final Report for USGS, Aerojet-General Corp., El Monte, Calif.

5. Hanson, B., 1975, Freeze-thaw experiment field data: RSL Technical Memorandum 177-53, Remote Sensing Laboratory, University of Kansas Center for Research, Inc., Lawrence, Kansas.

6. Katibah, Edwin F., 1975, Operational use of LANDSAT imagery for the estimation of snow areal extent: Operational Applications of Satellite Snowcover Observations, NASA SP-391, p. 129-142.

7. Limpert, Fred A., 1975, Operational Application of Satellite Snowcover Observations - Northwest United States: Operational Applications of Satellite Snowcover Observations, NASA SP-391, p. 71-86.

8. Linlor, W. I., J. L. Smith, M. F. Meier, F. C. Clapp and D. Angelakos, 1975, Measurement of snowpack wetness: Proc. 43rd Annual Western Snow Conference, San Diego, California.

9. Linlor, W. I., 1972, Snowpack water content by remote sensing: Intl. Symp. on Role of Snow and Ice in Hydrol., UNESCO-WMO, Banff, Canada, Sept. 6-20.

10. Moore, R. K., 1972, Use of microwave for snow, freeze-thaw and soil moisture determination -- a needed research program: RSL Technical Memorandum 100-1, Remote Sensing Laboratory, University of Kansas Center for Research, Inc., Lawrence, Kansas.

11. Schneider, Stanley R., 1975, The operational program of satellite snowcover observations at NOAA/NESS: Operational Applications of Satellite Snowcover Observations, NASA SP-391, p. 87-102.

12. Seifert, R. D., R. F. Carlson, D. L. Kane, 1975, Operational applications of NOAA-VHRR imagery in Alaska: Operational Applications of Satellite Snowcover Observations, NASA SP-391, p. 143-156.

13. Stiles, H., F. T. Ulaby, B. C. Hanson, and L. F. Dellwig, 1976, Snow backscatter in the 1-8 GHz region: RSL Technical Report 177-61, Remote Sensing Laboratory, University of Kansas Center for Research, Inc., Lawrence, Kansas, June.

14. Useful application of earth-oriented satellites: Hydrology, Summer Study, Panel 3, National Academy of Science, Washington, DC, 1969.

15. Waite, W. P. and H. C. MacDonald, 1970, Snowfield mapping with K-band radar: Remote Sensing of Environment, vol. 1, pp. 143-150.

16. Warskow, W. L., T. T. Wilson, Jr., and K. Kirdar, 1975, The application of hydrometeorological data obtained by remote sensing techniques for multipurpose reservoir operations: Operational Applications of Satellite Snowcover Observations, p. 29-38.

17. Washicheck, Jack N. and Tony Mikesell, 1975, Operational applications of satellite snowcover observations in Rio Grande drainage of Colorado: Operational Applications of Satellite Snowcover Observations, NASA SP-391, p. 53-70.

18. Vickers, R. S. and G. C. Rose, 1972, High resolution measurements of snowpack stratigraphy using a short pulse radar: Proc. Eighth Intl. Symp. on Remote Sensing of the Environment.

APPENDIX C

RSL TECHNICAL REPORT 295-3

VOLUME III

THE UNIVERSITY OF KANSAS SPACE TECHNOLOGY CENTER
Raymond Nichols Hall

2291 Irving Hill Drive—Campus West Lawrence, Kansas 66045

Telephone:

RADAR DETECTION OF WATER BODIES

RSL Technical Memorandum 295-5
Remote Sensing Laboratory

Bradford C. Hanson

January, 1976

Supported by:

NATIONAL AERONAUTICS AND SPACE ADMINISTRATION
Goddard Space Flight Center
Greenbelt, Maryland 20771

CONTRACT NAS 5-22384

ABSTRACT

Flood plain and flood inundation mapping, surface water mapping including estuary and wetland surveys, and flood area assessment has received considerable attention during the past decade because of man's increasing environmental awareness. Great strides have been achieved in creating new, more efficient methods for monitoring these parameters; most apparent are the innovations resulting from the ERTS and the SKYLAB programs. Active microwave sensors possess an even greater potential due to their independence of the operational constraints inherent to visible light-IR systems and their resolution superiority over passive microwave systems. An orbital platform containing a synthetic-aperture radar system would provide an additional, extremely valuable, tool for any water resource mapping program.

Optimum system parameters required for maximum data retrieval are difficult to establish due to an inadequate research data base. Based on radar theory and existing limited research, the following recommendations are submitted as realistic sensor instrumentation requirements:

frequency:	X-band
polarization:	HH
depression angle limitation:	less than 75^{o}
resolution:	12 meters
revisit time:	6 days

1.0 INTRODUCTION

Water percolates downward, displacing interstitial air within the zone of aeration until all pores are permeated. With additional moisture, downward infiltration will be impeded if the soil is in a state of maximum saturation. Additional surface water under these conditions exists either at the air-soil interface as free-standing water, or becomes runoff. Excessive amounts of the latter often cannot be contained within the confines of the river channel; when a drainage system can no longer accomodate the increased volume, flooding occurs. Floods are an extreme case of surface water runoff, but for any water resources management program, the ability to accurately identify and map flooded areas, and delineate those areas of potential flooding is of prime importance.

Most surface-water runoff is contained within a given drainage system or is entrapped by an inland water body, the latter comprising reservoirs, lakes, ponds, etc. Surveys involving the measurement of the total area of surface water over wide regions, continental or global, would be of scientific as well as practical use. The amount of water subject to evaporation, population-center accessibility to a water supply, more accurate indices of the total water available for consumption and its change with respect to time, would be more rapidly obtained utilizing remote sensing techniques. Volume information is of equal importance. Volumetric data can be utilized in the analysis of a local/regional water table, a parameter indicative of the water storage capacity for a particular area. Thus an equally important factor in a water resources management program is the ability to chart and measure surface water (lakes, ponds, marshes, etc.) on a local and on a regional basis and at regular intervals. The latter stipulation is necessary if monitoring changes with respect to time are to be realized.

The purpose of this paper is twofold: (1) to explore the potential use of an active microwave sensor to delineate various surface water phenomena and (2) to identify the proper radar design parameters for a system operating from an orbital platform.

2.0 PREVIOUS INVESTIGATIONS

Many investigations [Anderson, et al., 1973; Klemas, et al., 1973; Mairs, et al., 1973; Reeves, 1973] have dealt with flood plain and flood inundation mapping, surface

water mapping and flood area assessment including estuary and wetland surveys utilizing ERTS-1 data. Extensive work has been performed using ERTS because the images are readily attainable and because open areas of surface water are easily delineated by their strong contrast with the surrounding land mass at 0.8 - 1.1 μm. The major drawbacks have been the rather long repeat cycles of 18 days (9 days now possible with two satellites), resolution restrictions [Reeves, 1973] and restrictions imposed by inclement weather conditions during daylight hours. Other problems arise when considerations of wetland mapping are involved. It is not always possible to delineate with precision the marsh-water interface and the upper wetland boundary though certain plant communities may be useful for this [Anderson, et al., 1973; Klemas, et al., 1973; Mairs, et al., 1973].

Radar imaging systems are not restricted by the problems previously discussed. Daylight operation is no longer a restriction with radar, nor does cloud cover impede data retrieval. Moreover, fine resolution is achievable from any altitude since resolution is independent of range for a synthetic-aperture radar. An added benefit is its ability to delineate physiographic characteristics which might otherwise go unnoticed on aerial photography (Figure 1). Note the channel configuration and the associated meander scars; surface features such as soil variations, agricultural patterns, vegetation, and land use boundaries are also vividly expressed. Note also that intra-channel physiographic features such as mudflats are discernable to a certain degree from the surrounding mass of water.

Radar has been suggested as a useful tool for the detection and mapping of inland water bodies as far back as 1967 [McCoy, 1967] due to its characteristic appearance on imagery. Roswell [1969] concluded that lakes larger than 8 acres in area could be detected in well drained, lowland areas on AN/APQ-97 imagery; Simpson [1969] obtained similar results for an area in New England.

Radar (X-band) has been utilized for flood warning and damage assessment on a very limited basis. Rydstrom [1970] presented several techniques for identifying flooded areas. He noted the strong contrasts in returns between flooded and non-flooded fields and that breaks in levees were identifiable due to a disruption in the high return generated from the levee. Dams and associated spillways displayed high returns during normal pool, but during periods of high water when the spillway is active, no return is recorded for the spillway structure [Rydstrom, 1970].

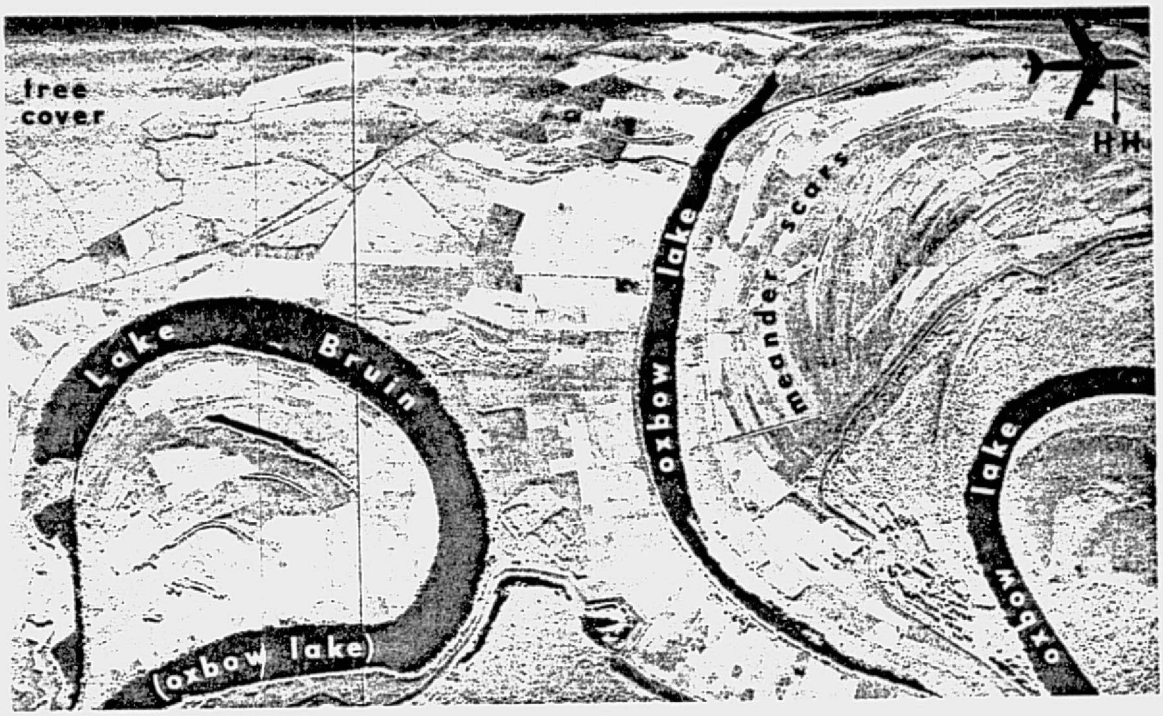

A

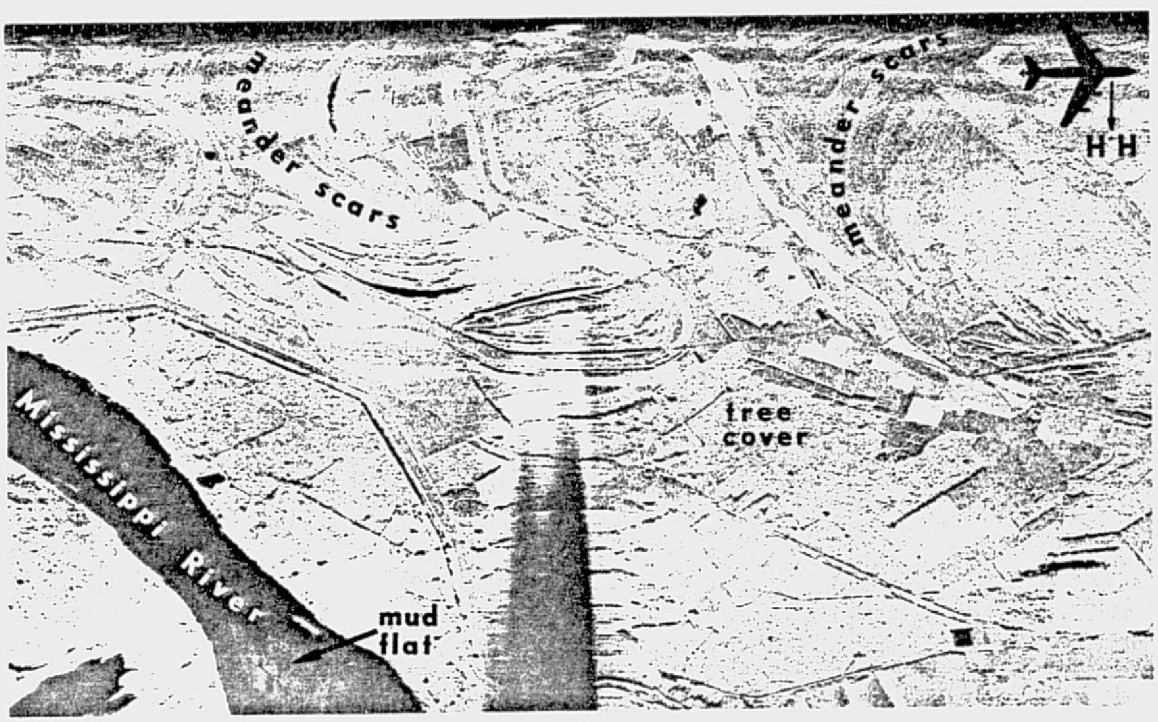

B

FIGURE 1. AN/APQ-97 radar imagery -- Mississippi River Valley near Vicksburg, Mississippi.

3.0 RADAR SIGNAL RETURN

Depending on the relative roughness of the terrain, the radar return signal from vegetation, soil, rock, etc. is generally greater than the return signal from water. Radar signals are normally returned from the terrain to the receiver by a scattering process (reradiation) with the intensity of radar return (signal strength) from the terrain determining the relative degree of brightness on the radar image. Parameters that influence radar return are frequency, polarization, complex dielectric constant, incidence angle, and surface roughness.

The local angle of incidence, θ, is the angle formed between an impinging beam of radar energy and a perpendicular to the imaged surface at the point of incidence (Figure 2A). The angle between a line from the transmitter to a point on the terrain, and a horizontal line passing through the transmitter is the depression angle (α). On flat terrain there is a continuous change in the angle of incidence from a maximum at far range to a minimum, near normal incidence, in the near range. This relationship is modified with the introduction of a slope to the terrain surface (Figure 2B).

The energy incident on a horizontal terrain surface is "specularly" and/or "diffusely" reflected in varying proportions depending upon the roughness of the terrain. Surface roughness is a geometric property of the terrain expressed relative to wavelength. Surfaces with micro-relief much less than a quarter-wavelength appear smooth (no return) whereas surfaces with micro-relief on the order of a wavelength or more, appear "rough". A smooth surface is characterized by specular or mirror-like reflection with the angle of incidence determining the orientation of the reradiation pattern (Figure 3A). Under these conditions, the reflection obeys Snell's Law (angle of incidence equals angle of reflection) with virtually all the reflected energy being contained within a small angular region about the "specular" angle. When water bodies such as lakes and rivers are imaged, they act as near-specular reflectors and as such direct most of the transmitted energy away from the receiver (Figure 4B) except near vertical incidence ($\theta = 0^{\circ}$) where strong backscatter is recorded (Figure 4A). Numerous investigators have noted a strong return in the extreme near range (maximum depression - minimum incidence angle) for ocean surfaces (Figure 5A); however, most energy is reflected away from the radar for incidence angles exceeding 10 to 15 degrees [Hanson and Dellwig, 1973].

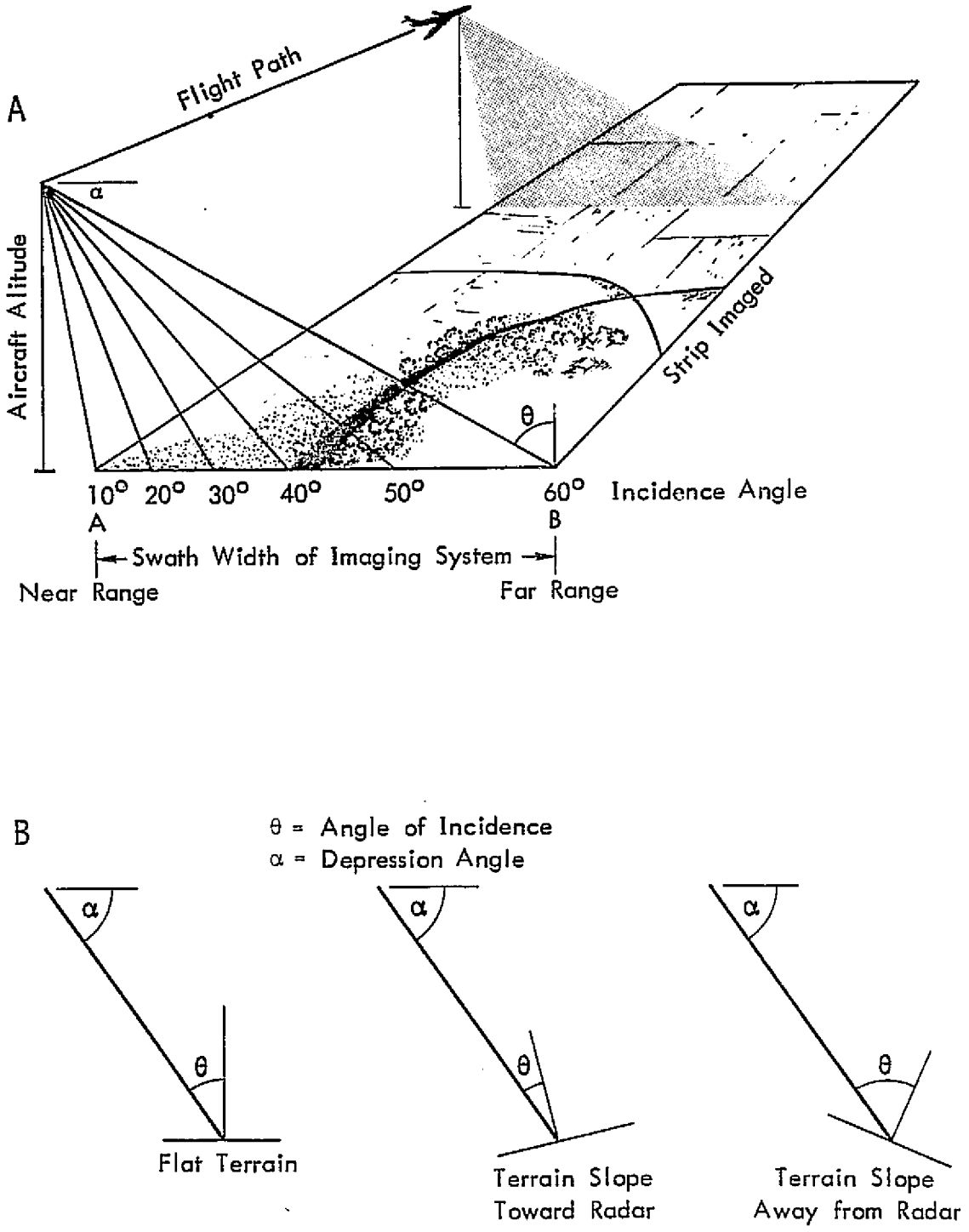

FIGURE 2. THE RELATIONSHIP BETWEEN ANGLE OF INCIDENCE, DEPRESSION ANGLE, AND TERRAIN SLOPE.

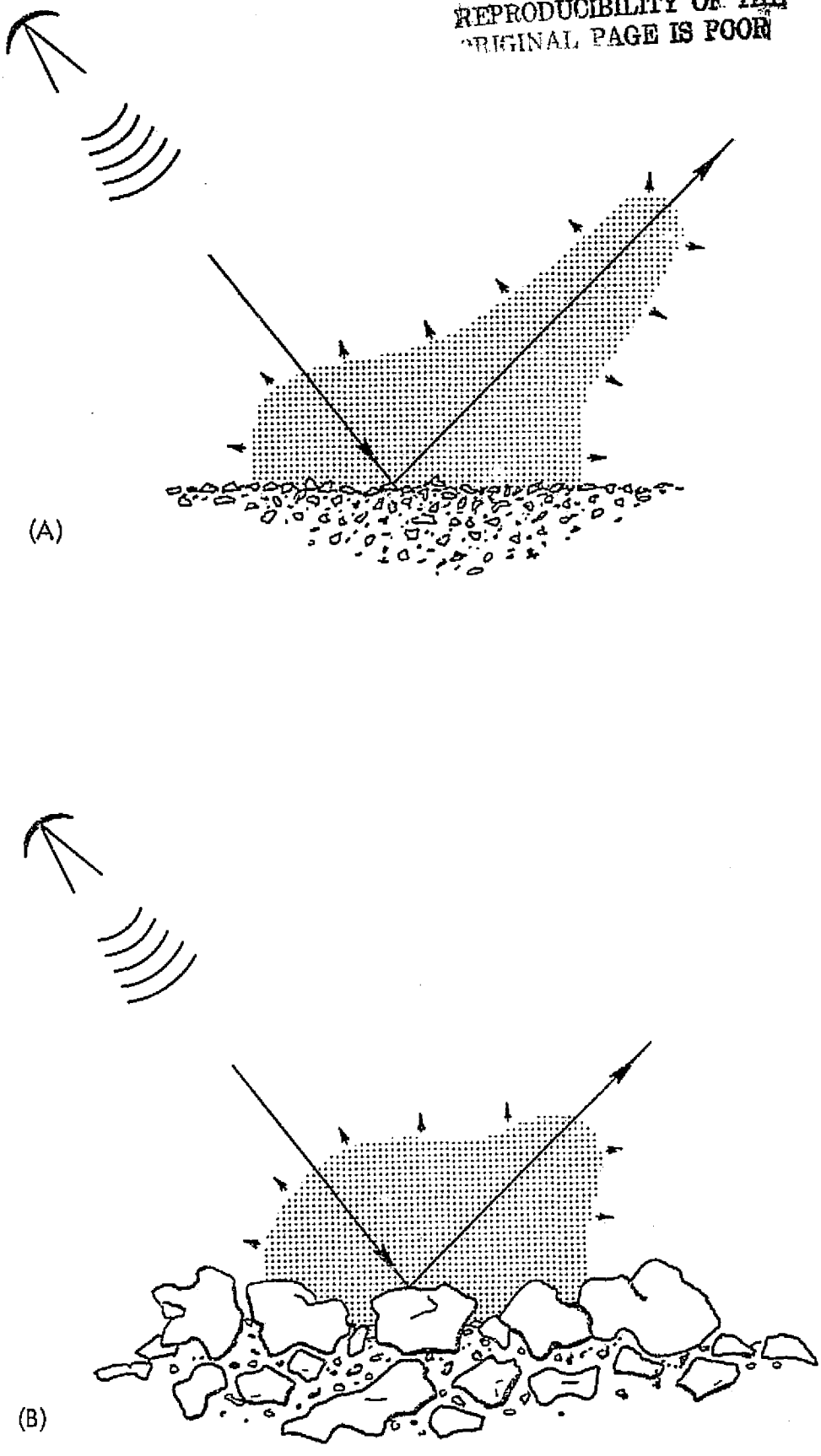

Figure 3.

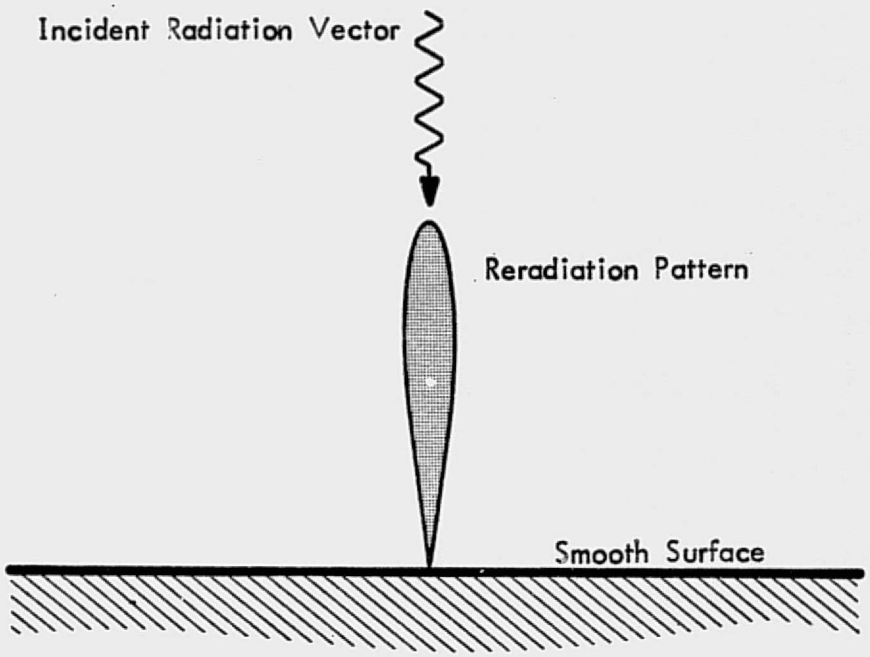

A. Normal Incidence

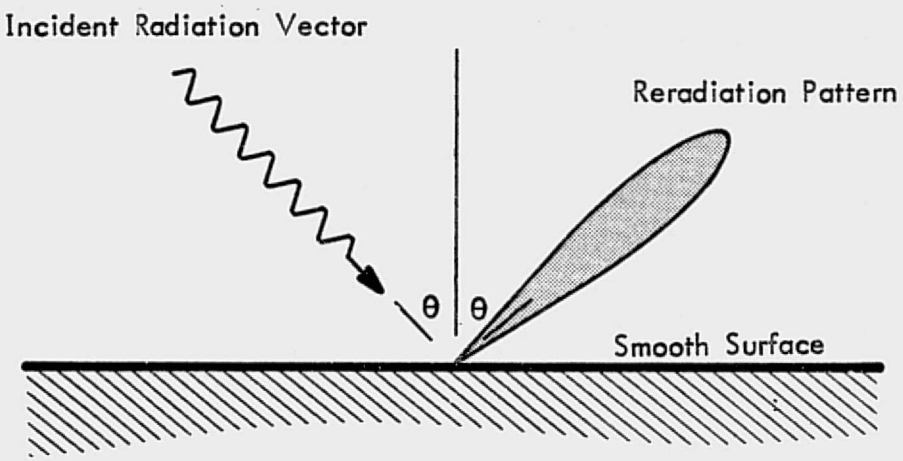

B. Oblique Incidence

FIGURE **4.** APPROXIMATE RERADIATION PATTERN FOR REFLECTION FROM A SMOOTH SURFACE.

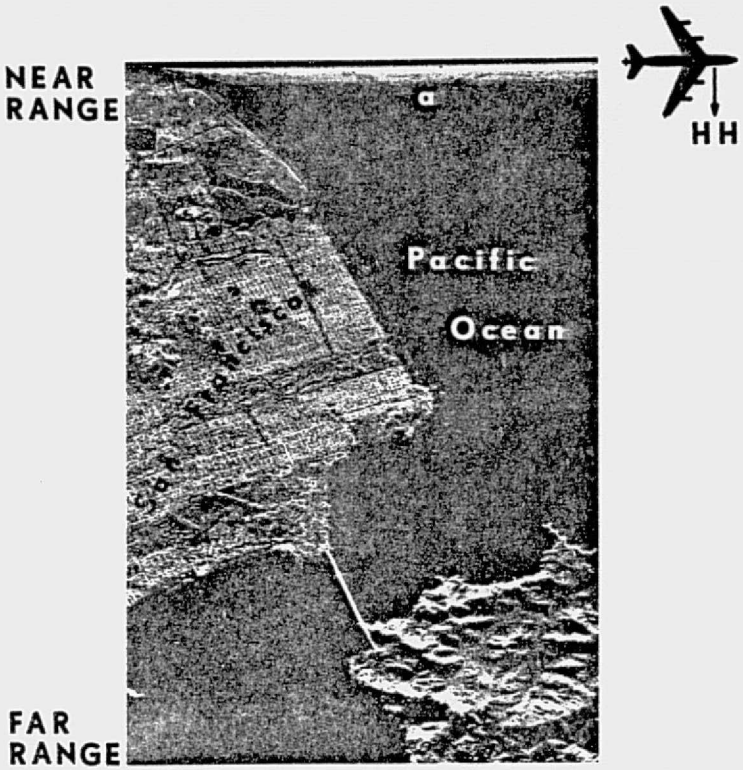

FIGURE 5. AN/APQ-97 radar imagery -- Golden Gate area, San Francisco, California.

The scatter of radar signals from disturbed water surfaces is usually less than that from land, but can be a confusing factor in distinguishing land-water boundaries. Backscatter from waves is governed largely by the height of the wind-driven capillary waves, with modulation by the tilting of these tiny wavelets by the larger waves. When the wind is high, the backscatter approaches that from land in strength. Within 15° or so of the vertical, the role of the capillary waves diminishes and the return (much stronger than at larger angles) is determined by the larger waves. The typical variation of radar return in an image is indicated in Figure 6A, B, C, A; in Figure 6D no return is observed in the near zone, probably because of a very calm surface.

The strength of returns from water is important from the standpoint of surface water mappability. For example, area and volumetric information can only be realized if the shoreline for a particular water body can be delineated. Under certain circumstances, shoreline recognition and mapping would be impeded if the area under investigation was situated in the extreme near range; accuracy in shoreline location would be minimal due to a high return from both the land and the surface of the water (Figure 7; A).

The discussion thus far has been concerned with high microwave frequencies, on the order of 10 GHz to 35 GHz, X-band to Ka-band. Existing limited research, compiled at these frequencies, suggests that any microwave frequency between these two end-points will suffice for detecting and mapping free-standing water (lake, reservoir, pond, etc.) within a system's resolution capability. Decreasing the frequency usually causes a surface to appear smoother; smoothing the effects of surface roughness instigates a decrease in the amount of energy backscattered by a target. For water the effect would be a decrease in the signal return at incidence angles greater than zero degrees even though the physical characteristics of the capillary waves remained constant. Thus it may be possible to override the effects of increased radar return due to the capillary waves and hence may be possible to reduce the problem discussed for Figure 7. Unfortunately, comparative imagery, L-band versus a higher frequency system such as X-band, was not available for our study to either confirm or discount this contention.

One study was undertaken to determine the feasibility of utilizing multiplexed, synthetic-aperture X- and L-band radar to obtain specific data over varying terrains [Drake et al., 1974]. For the purpose of water resources management, their analysis indicated that X-band imagery permits identification of small nonlinear and

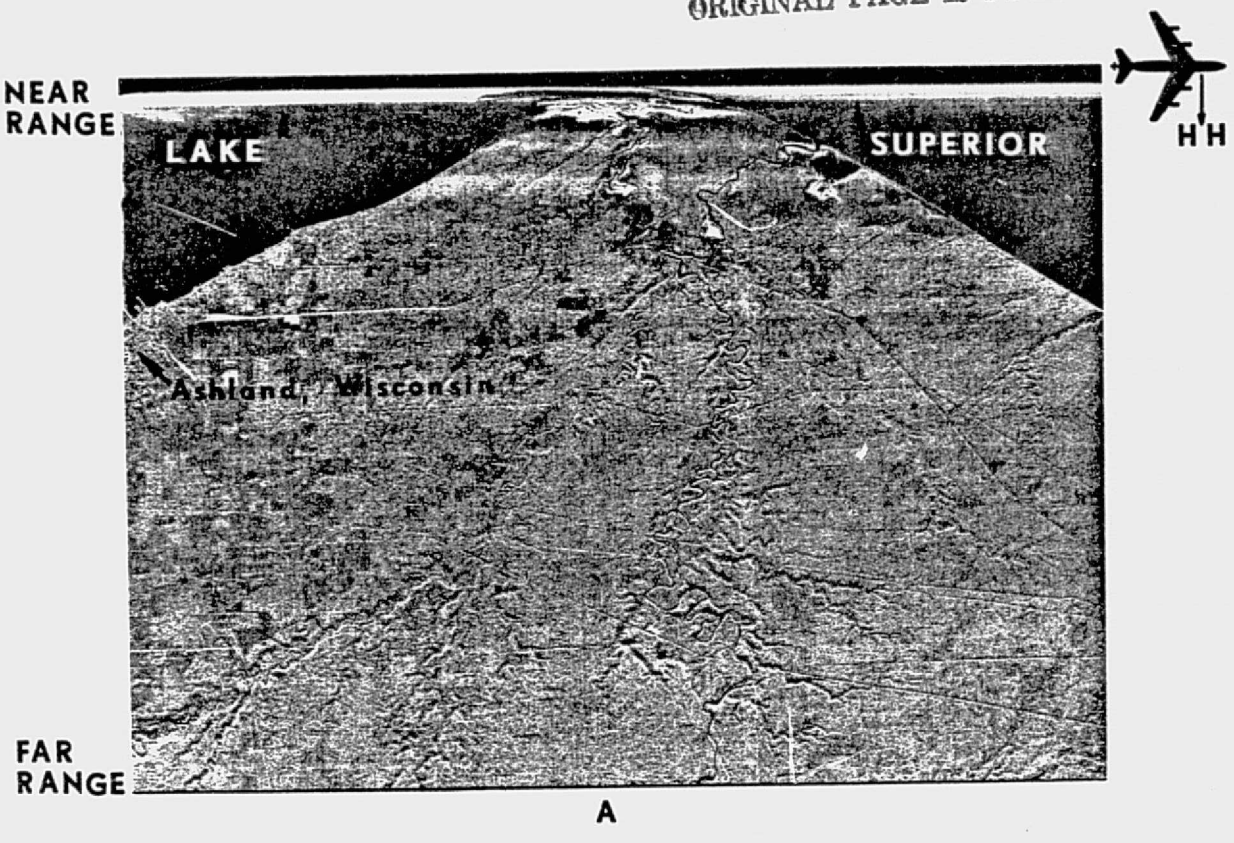

FIGURE 6. AN/APQ-97 radar imagery illustrating radar return variations for water bodies in the extreme near range.

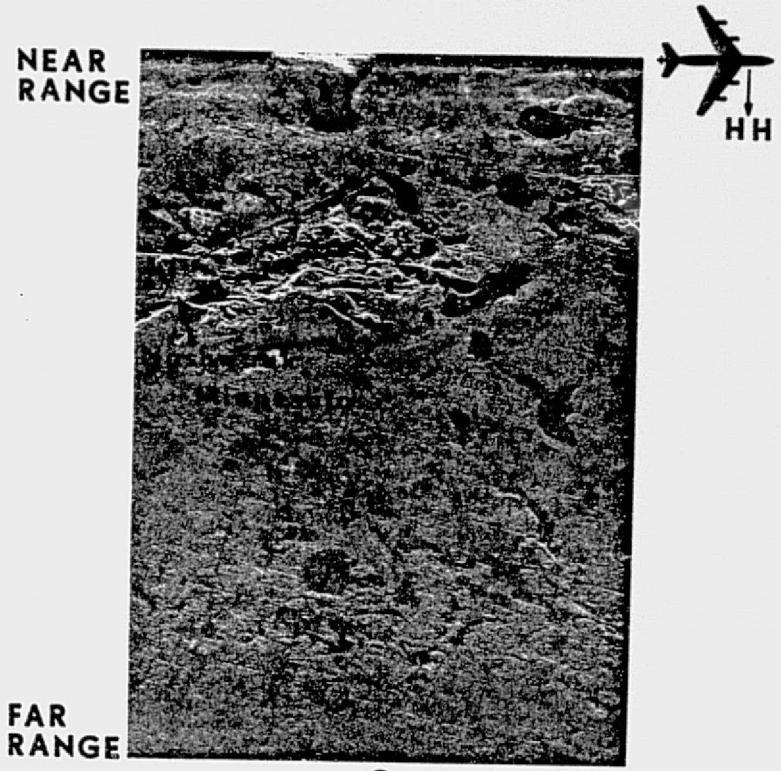
NEAR
RANGE
HH
FAR
RANGE

C

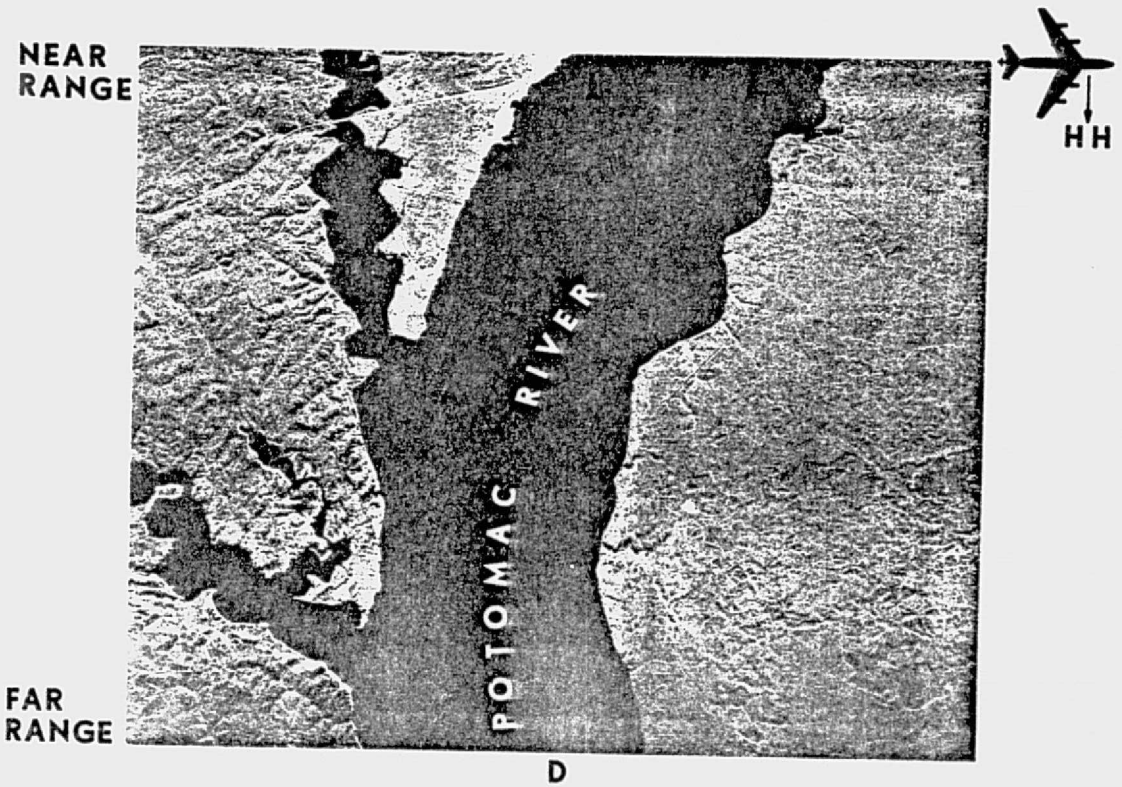
NEAR
RANGE
HH
POTOMAC RIVER
FAR
RANGE

D

FIGURE 6.

FIGURE **7.** Shoreline recognition and mapping impedance for water bodies imaged in the extreme near range (AN/APQ-97).

narrow linear open water areas; L-band imagery exhibited a more subdued response to these features which often rendered the imagery useless for identification purposes. Analysis of shorelines indicated that radar at X-band and shorter wavelengths was superior to L-band imagery in every respect; shoreline delineation is ambiguous when the peripheral vegetation is low and of even height when imaged with an L-band system, but is easily located on X-band imagery [Drake et al., 1974]. Pads of water lilies are faintly indicated on both X- and L-band imagery as well as hyacinths and to some degree reeds; differentiation is only possible by utilizing both polarizations (like and cross) [Drake et al., 1974].

The radar return generated for flood inundated areas at differing frequencies should depend upon the surface characteristics of the water, the nature of any floating materials, and whether all ground cover is completely submerged, or whether some is protruding above the surface of the water. At low frequencies, for example, radar return for inundated areas with considerable floating surface material (logs, trees, etc.) or an area in which surface water does not totally conceal all ground cover (similar to a marshy condition), may differ considerably from that generated by a higher frequency system such as Ka-band. Moreover, it has often been noted that islands could not be positively identified from masses of floating vegetation at either X-band or L-band frequencies [Drake et al., 1974].

The boundary between swamp or marsh and open water presents a different problem; Roswell [1969] observed that the boundary is often diffuse. He noted that the gradation of gray tones between open water, water/vegetation intermixing, and non-water surfaces creates difficulties when establishing definite boundaries. The area exhibiting high return (Figure 8A; Areas X) peripheral to the river are wetlands dominantly vegetated by the common reed, Phragmities communis, interspersed by Wild Rice, Zizania aquatica. The vegetation dominant in the areas of moderate return characterized by the speckled texture (Figure 8A; Areas Y) is that of tall, slender Bluejoint grass. Both vegetation habitats generally exhibit definite, recognizable boundaries relative to each other and to the land-water interface. An exception to the latter occurs where water and sparse vegetation are intermixed (Figure 8A; A) thus creating a zone of transition. Definite boundaries are easily established for terrestrial vegetation habitats where plant diversity is prevalent. For example, Areas Z (Figure 8A) are dominated primarily by Black Spruce, Picea mariana, of uniform height (approximately 6 meters) and density. These areas are

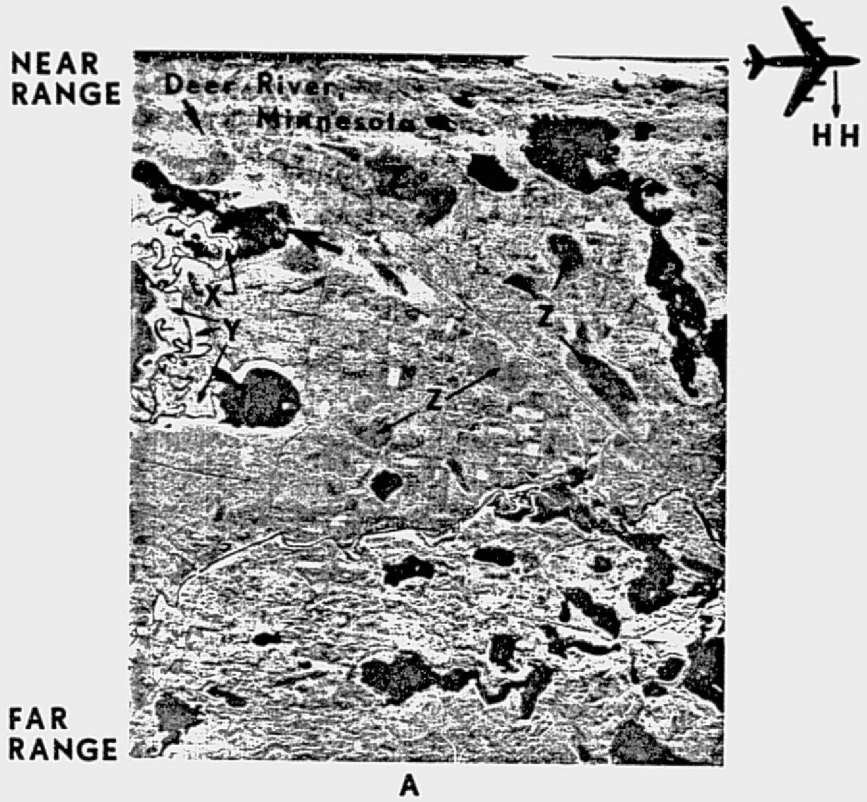

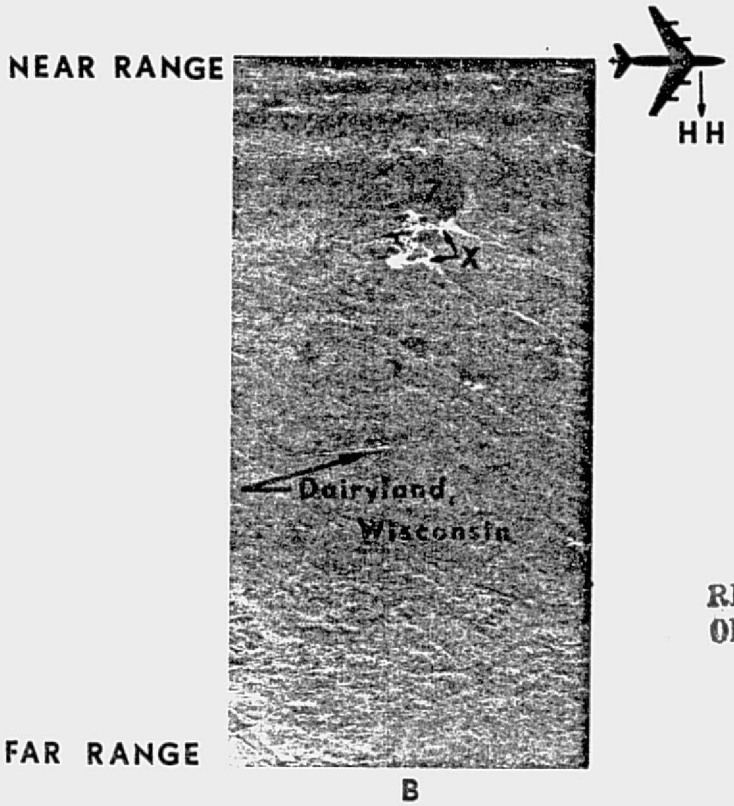

FIGURE **8.** AN/APQ-97 radar imagery illustrating return variations for marsh and wetland regions.

easily delineated from the surrounding vegetation (primarily deciduous forest) by their lower radar return intensities and from nearby water bodies by their textural characteristics. The same observation holds when considering marsh areas dominated by Black Spruce in other locales (Figure 8B; Area Z). Moreover Area X (Figure 8B) is primarily Bluejoint grass interspersed with the common reed and intermixed by minor amounts of wild rice. Thus it appears that definite boundaries can be established in most instances, the exception being water intermixed by sparse vegetation. The effect of incidence angle on such discriminations is unknown.

Observations by Drake and others [1974] indicate that strong returns from marsh areas on X-band imagery are reflections from the top of the vegetation. At L-band frequencies, penetration apparently occurs; marsh reeds up to 5 feet above the surface of the water are penetrated, resulting in specular reflection. One further observation was noted: marsh areas were often confused with certain types of rangeland and agricultural land on both L-band imagery and X-band imagery but especially the latter. It must be noted however, that the observations by Drake [1974] were performed on test sites located in Brevard County, Florida; vegetation differs dramatically with respect to its physical size, shape, and other characteristics depending upon region. Hence, vegetation characteristic to a marshland in Florida may not be the same as that which is characteristic of marshes in other parts of the country. Thus, observations for marshlands in Florida may or may not hold for marshes in northern Minnesota.

The low return observed for Figures 8A and 8B, Area Z, is the result of the vegetation characteristic to these environmental niches; the Black Spruce of uniform height and density has created a smooth surface relative to the wavelength involved, hence the low return. The high return noted for Figures 8A and 8B, Area X and the moderate radar return observed for Area Y is due to differences in vegetation. For example, the Reed grass, Phragmities communis, are erect plants which vary from 2 meters to 4 meters in height, possess flat blades 1 cm to 5 cm wide and 15 cm to 40 cm long, grow in dense clusters, and are often confused with wild rice (Fassett, 1940). Even though the water level was 2.7 feet above normal pool (U.S. Corps of Engineers, Grand Rapids, Minnesota) when the radar image was flown (October 15, 1965), the strong radar return (Figure 8A; Area X) is the result of backscatter from the plant community; these stout, erect plants were partially submerged but retained their density and physical characteristics above the surface of the water. The more moderate

return intensities from the Bluejoint grass thought to be Calamagrostis canadensis (Figure 8A; Area Y), is also the result of backscatter from the vegetation. Bluejoint are tall, slender grasses, seldom exceeding 2 meters in height, possess flat blades less than 1 centimeter wide and 20 cm to 40 cm long and often form dense ground covers (Fassett, 1940). When partially submerged however, the Bluejoint grass does not produce a radar return signal as strong as that for the Phragmities community because the canopy of Bluejoint grass above the surface of the water is not as dense and thereby probably permitting a small portion of the impinging radar signal to be reflected from the water surface.

Frequency is a parameter which also appears to control the degree of backscatter observed for different topographic situations. For marsh and wetland areas in Florida, L-band appears superior to X-band because of its penetration capability; for open water areas and shoreline delineation, X-band is a better choice [Drake et al., 1974]. For similar areas in northern Minnesota, microwave frequencies lower than X-band may create boundary problems. In the case of Area Z (Figure 8A), lowering the microwave frequency may result in an obscured boundary since longer wavelengths tend to smooth surface features; hence differences in radar return are more subdued. For areas where diffuse boundaries are a problem, lowering the frequency often results in a more clearcut situation; differences between the non-water surface and the intermixing zone become less evident and when compared to the open water zone a definite boundary becomes apparent [Roswell, 1969]. Thus there appears to be a tradeoff in retrievable data when considering frequency.

Polarization has no pronounced effect on the image brightness from open water except at near range depression angles (Figure 9-10; A) with usual over-land gain settings because returns of both polarizations appear black. However if the gain were set high enough to image signals from the water surface, VV signals would be much brighter than HH or cross-polarized signals. Marsh areas (m) dominated by the Black Spruce and wetland regions (w) dominated by grasses (Figures 11-12) exhibit strong variations in the degree of returned energy for different polarizations (HH or HV) at Ka-band frequencies. One area (Figures 11A and 11B; Areas X) exhibits tonal reversals opposite to that observed for the wetland regions and marsh areas. On like (HH) polarized radar imagery (Figure 11A; Areas X), the radar return is comparable to the surrounding deciduous forest but on cross (HV) polarized

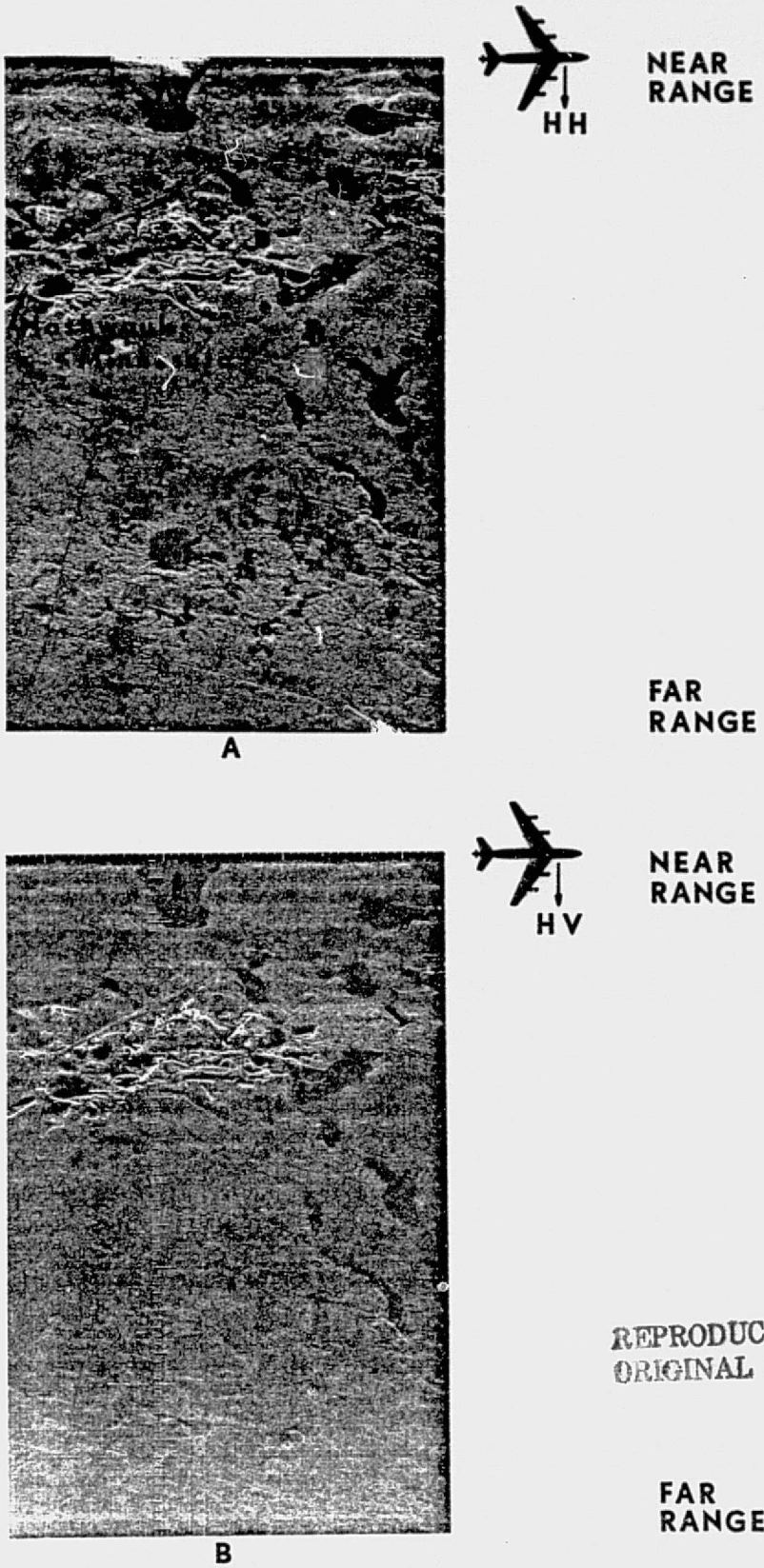

FIGURE **9.** AN/APQ-97 radar imagery showing polarization effects on open water in the extreme near range.

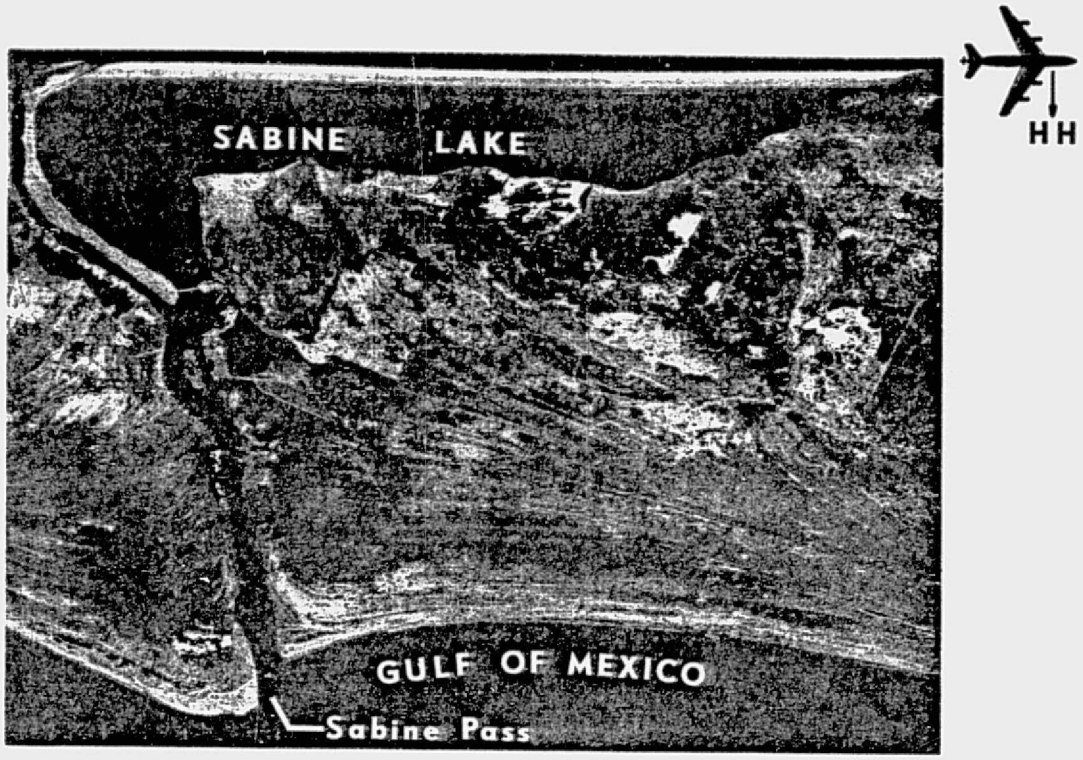

A

B

FIGURE **10.** AN/APQ-97 radar imagery showing polarization effects on open water in the extreme near range.

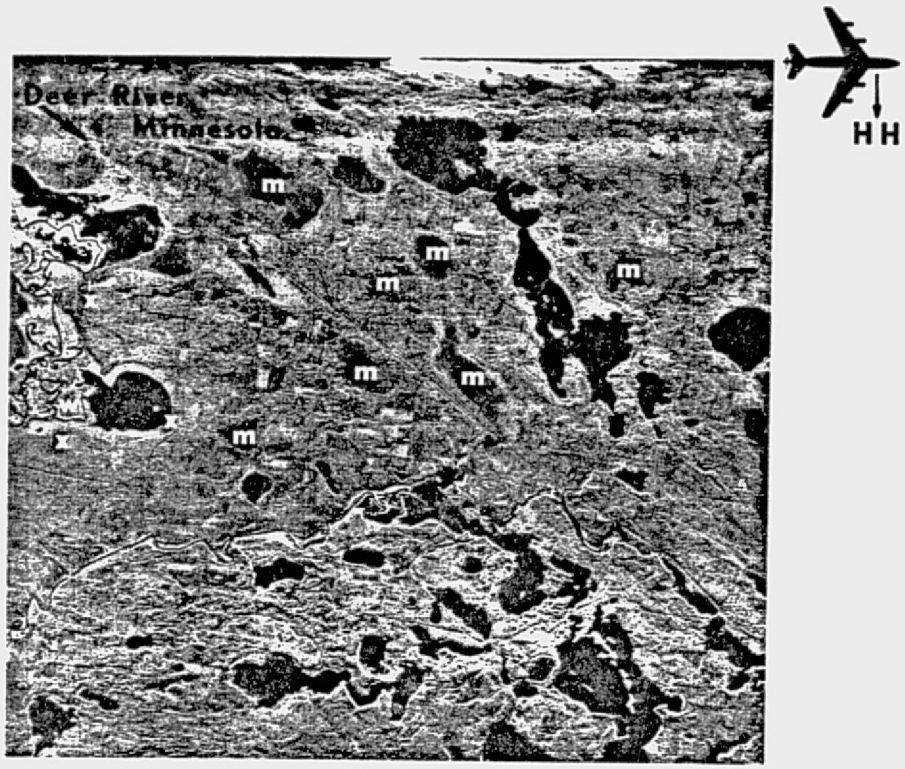

A

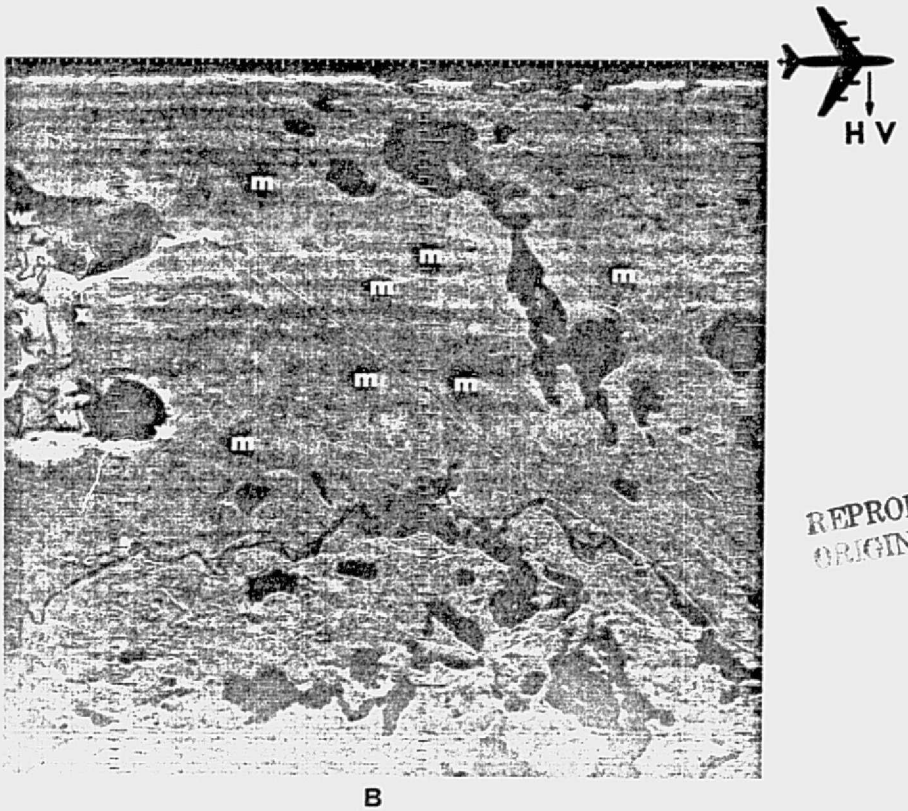

B

FIGURE **11.** AN/APQ-97 radar imagery depicting tonal reversals for like (HH) and cross (HV) polarization of wetland (w) and marsh (m) regions.

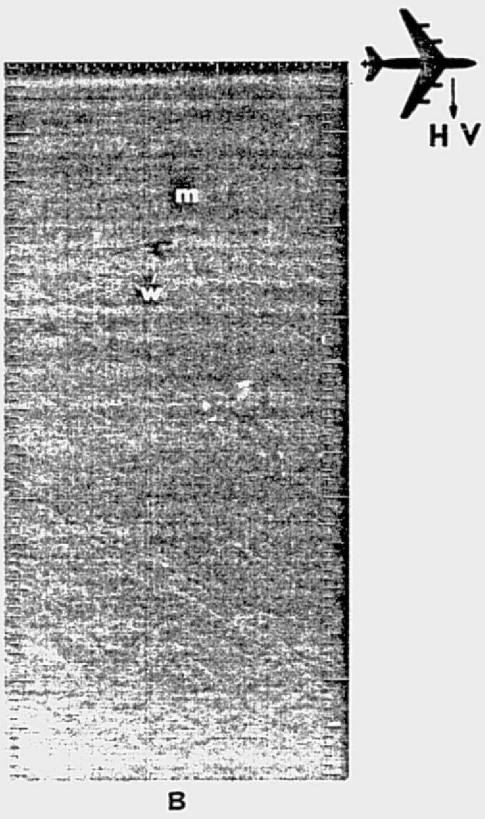

FIGURE **12.** AN/APQ-97 radar imagery depicting tonal reversals for like (HH) and for cross (HV) polarization of wetland (w) and marsh (m) regions.

imagery (Figure 11B; Areas X) these same locales exhibit high radar returns. The vegetation is principally sawgrass which belongs to the Sedge family, Cyperaceae, and is thought to be of the large and complex genus Carex. It is postulated that the cross (HV) polarized radar signal undergoes volume scattering, thereby producing the anomalous high return. This strong depolarization occurs only for areas dominated by the Carex. Presumably this relates to the tendency of Carex to "droop" when standing in water, while the other species observed remain more erect.

It has been noted by previous investigators [MacDonald and Waite, 1971] that like-polarized imagery provides maximum differentiation at K-band wavelengths; Batlivala and Ulaby [1975] observed that polarization had little effect on the moisture response for bare ground for low microwave frequencies between 2 GHz and 8 GHz. However, wetland areas and marshy conditions were not considered in the latter investigation. Operating at frequencies lower than X-band for marsh delineation and for estuary and wetland surveys may or may not require polarization consideration.

Thus far, the discussion has centered on free-standing water such as reservoirs or ponds, marshes and wetland regions, and flood inundated areas which are not covered by forest canopies. Pools of water beneath vegetation and particularly under canopies of dense vegetation cannot be detected with either X-band or L-band radar for moderate and low depression angles [Drake et al., 1974]. Moreover, several studies at K-band frequencies [MacDonald, 1969; Wing, 1971; Moore, 1971] indicate that penetration does not occur and that the return is from the top of the tree canopy. Barr and Miles [1970] observed higher radar returns from vegetation, especially low vegetation, peripheral to pools of water and concluded that it was the result of vegetation with a higher moisture content, which is consistent with controlled observations of vegetation backscatter [Ulaby, 1975]. Thus it may be possible to indirectly detect pools under dense vegetation.

It is apparent that detection of water under a dense canopy is impossible at moderate and low depression angles; steep depression angles, where the angle of incidence approaches 0°, may provide necessary penetration capability depending upon the canopy characteristics. For example, by increasing the wavelength from

0.86 cm to about 20 cm (Ka-band to L-band), the attenuation is decreased and therefore greater penetration of the overlying canopy may be possible. However, it must be remembered that as the angle of incidence approaches zero, strong backscatter is recorded from smooth surfaces which not only can create the interpretation problems as discussed for Figure 7, but may also result in the similar return intensities originally observed at moderate and low depression angles. Thus, another trade-off appears to exist when considering depression angle.

A final category for discussion concerns flowing water. Much information can be gathered on sub-surface topography by noting the surface flow characteristics. Radar may have a potential application if the system could be designed such that small scale flow patterns could be observed. A low frequency system would probably be unacceptable since it would tend to smooth the very features necessary for any analysis. An adequate resolution cell should be equivalent to about one-fourth of the width of the river. For major drainage systems, 50 meter resolution is not unrealistic; for smaller rivers a resolution of about 10 meters should provide adequate detail. For shoreline analysis including deltaic phenomena, the latter resolution requirement should provide the maximum amount of detail required for most interpretations.

4.0 CONCLUSIONS

The optimum system parameters are difficult to establish at this time since little research has been undertaken to provide adequate data on sensor responses to land-water boundaries under differing physical conditions.

Incidence angle (depression angle) considerations are an important parameter from the standpoint of signal return from open water. To insure accurate shoreline delineation and eliminate the problem illustrated in Figure 7, a limitation in the depression angle should be established at 75°. This limitation may or may not provide the necessary penetration capability needed for pool detection under vegetation canopies. A major control parameter will be vegetation density.

An average revisit time of not more than 6 days is suggested as a compromise for lakes, ponds, and estuaries (size of feature and type of data requested obviously control periodicity of coverage needed); wetlands require less frequent coverage, from 30 days to 1 year depending upon their physical size. For flood plain delineation, channel characteristics, etc., periodic coverage each year would suffice, while

flood damage assessment requires coverage upon demand (periodicity of coverage obtained from tables of measurable parameters from a report entitled "Satellite Data Collection User Requirements: Report of the NASA Ad Hoc Committee on Hydrology"). Thus as illustrated above, revisit time can fluctuate depending upon the feature for which data is recorded. To insure adequate periodic coverage for all surface water phenomena, a revisit cycle of 6 days is suggested as a compromise, but a system should be capable of "pointing" to flooded areas on demand.

Polarization is an important parameter for water surfaces imaged at steep depression angles, the extreme near range. Cross-polarized imagery (HV) however, subdues the radar response to marshy areas. The least complicated solution appears to be the utilization of like-polarized (HH) imagery at depression angles shallower than those generating the problem response in the near range. However, the use of dual polarization (HH and HV) allows for better identification of vegetational differences within wetland regions.

Based upon existing radar imagery viewed by this investigator, a proposed system resolution of approximately 12 meters should provide sufficient information for both regional analyses and provide for local detail, although finer resolution would produce greater detail. Additional data should be acquired however to quantify this requirement; one such investigation was conducted by Moore and Dellwig [1976] for a variety of target types.

Frequency will control the radar responses observed for any given target. Past investigations have dealt primarily with X-band and K-band imaging systems. Based on the limited research data base existing for water body detection, L-band does not appear to possess advantages over higher frequency systems and in many cases, as previously discussed, resluted in serious limitations. Unfortunately, data is not available for S-band or C-band imagery, thus it is impossible to determine its feasibility for monitoring the features discussed above.

Based on available research, the following recommendations are proposed:

frequency:	X-band
polarization:	HH
depression angle limitation:	less than 75^{o}
resolution:	12 meters
revisit time:	6 days

In the opinion of the author, a system operating at 4 GHz (proposed system for soil moisture) should provide the necessary data without the disadvantages observed at L-band frequencies. This contention cannot, however, be substantiated with supportive data. Research is limited to a very few investigations at high frequencies and even fewer which utilize the lower frequencies. The obvious solution to the dilemma is research aimed at the whole surface water problem; research that will provide data for frequencies between L-band and K-band such that meaningful comparisons can be realized. A working ground-based research system exists whereby experimental data is retrievable for frequencies between 1 GHz and 18 GHz and over all the potentially useful incidence angles and polarizations; a major obstacle delaying such an investigation is project funding.

BIBLIOGRAPHY

1. Anderson, R. R., V. Carter and J. McGinness, Mapping Atlantic coastal marshlands, Maryland, Georgia, using ERTS-1 imagery: Symposium on Significant Results Obtained From the Earth Resources Technology Satellite-1, vol. 1, sec. A., Rpt. #E7, p. 603-614.

2. Barr, D. J., and Miles, R. C., 1970, SLAR imagery and site selection. Photogrammetric Engineering, vol. 36, no. 11, p. 1155-1170.

3. Batlivala, P. P. and F. T. Ulaby, 1975, Effects of roughness on the radar response to soil moisture of bare ground: University of Kansas Center for Research, Inc., Lawrence, Kansas, RSL Tech. Rpt. 264-5, 44p.

4. Claassen, J. P., A. K. Fung, S. T. Wu and H. L. Chan, 1973, Toward RADSCAT measurements over the sea and their interpretation: NASA Contractor Rpt., NASA CR-2328, National Aeronautics and Space Administration, Washington, D. C., 114p.

5. Drake, B., M. L. Bryan, C. L. Liskow, R. A. Shuchman, R. W. Larson, and R. A. Rendleman, The application of airborne imaging radars (L- and X-band) to earth resources problems: Radar and Optics Division, ERIM, Ann Arbor, Mich., Tech. Rpt. under Contract NAS10-8333, 83p.

6. Fassett, N. C., 1940, A manual of aquatic plants: McGraw-Hill Book Co., Inc., New York, 1st ed., 382p.

7. Hallberg, G. R., B. E. Hoyer and A. Rango, 1973, Application of ERTS-1 imagery to flood innundated mapping: Symposium on Significant Results Obtained From the Earth Resources Technology Satellite-1, vol. 1, sec. A., Rpt. #W5, p. 745-753.

8. Hanson, B. C. and L. F. Dellwig, 1974, Radar signal return from near-shore surface and shallow subsurface features, Darien Province, Panama: Proc. Am. Soc. Photogramm., Fall Convention, Part II, p. 1917-1931.

9. Klemas, V., F. Daiber and D. Bartlett, 1973, Identification of marsh vegetation and coastal landuse in ERTS-1 imagery: Symposium on Significant Results Obtained From the Earth Resources Technology Satellite-1, vol. 1, sec. A., Rpt. #E8, p. 615-628.

10. Lind, A. O., 1973, Application of ERTS imagery to environmental studies of Lake Champlain: Third Earth Resources Technology Satellite-1 Symposium, vol. 1, sec. B., Rpt. #W12, p.

11. MacDonald, H. C., 1969, Geologic evaluation of radar imagery from Darien Province, Panama: Modern Geology, vol. 1, no. 1, p. 1-63.

12. MacDonald, H. C. and W. P. Waite, 1971, Soil moisture detection with imaging radars: Water Resources Research, vol. 7, no. 1, p. 100-110.

13. Mairs, R. L., F. J. Wobber and D. Garofalo, 1973, Application of ERTS-1 data to the protection and management of New Jersey's coastal environment: Symposium on Significant Results Obtained From the Earth Resources Technology Satellite-1, vol. 1, sec. A, Rpt. #E9, p. 629-634.

14. McCoy, R. M., 1967, An evaluation of radar imagery as a tool for drainage basin analysis: CRES Tech. Rpt. 61-31, University of Kansas Center for Research, Inc., Lawrence, Kansas, p. 1 - 102.

15. Moore, R. K., 1971, Radar and microwave radiometry, in Proceedings, Int. Workshop on Earth Resources Survey Systems, Ann Arbor, SP-282, vol. 1, NASA Washington, p. 283-301.

16. Moore, R. K. and L. F. Dellwig, 1976, Final report on shuttle imaging radar studies: RSL Tech. Rpt. 287-1, University of Kansas Center for Research, Inc., Remote Sensing Laboratory, Lawrence, Kansas.

17. Morrison, R. B. and M. E. Cooley, 1973, Assessment of flood damage in Arizona by means of ERTS-1 imagery: Symposium on Significant Results Obtained From the Earth Resources Technology Satellite-1, vol. 1, sec. A., Rpt. #W6, p. 755-768.

18. Rango, A. and A. T. Anderson, 1973, ERTS-1 flood hazard study in the Mississippi River Basin: Third Earth Resources Technical Satellite-1 Symposium, vol. 1, sec. B, Rpt. #W10, p. 1127 - 1188.

19. Reeves, O. C., 1973, Dynamics of playa lakes in the Texas High Plains: Third Earth Resources Technology Satellite-1 Symposium, vol. 1, sec. B., Rpt. #W5, p. 1041-1070.

20. Roswell, C., 1969, Detectability of water bodies by side-looking radar: University of Kansas Center for Research, Inc., Lawrence, Kansas, RSL Tech. Rpt. 177-16, 46p.

21. Rydstrom, H. O., 1970, Flood warning and assessment assisted by high resolution radar: GIB-9200, Goodyear Aerospace Corp., Litchfield Park, Ar., 3p.

22. Simpson, R. B., 1969, Geographic evaluation of radar imagery of New England: Project in Remote Sensing, Dartmouth College, Hanover, New Hampshire.

23. Ulaby, F. T., 1975, Radar response to vegetation: IEEE Trans. Antennas and Propagation, Vol. AP-23, no. 1, p. 36-45.

24. Wing, R. S., 1971, Structural analysis from radar imagery of the eastern Panamanian Isthmus: Part I: Modern Geology, vol. 2, no. 1, p. 1-21.

APPENDIX D

RSL TECHNICAL REPORT 295-3

VOLUME III

THE UNIVERSITY OF KANSAS SPACE TECHNOLOGY CENTER
Raymond Nichols Hall
2291 Irving Hill Drive—Campus West Lawrence, Kansas 66045
Telephone:

RADAR MONITORING OF LAKE/RIVER ICE -- STATE OF THE ART

RSL Technical Memorandum 291-4
Remote Sensing Laboratory

S. K. Parashar

January, 1976

Supported by:

NATIONAL AERONAUTICS AND SPACE ADMINISTRATION
Goddard Space Flight Center
Greenbelt, Maryland 20771

CONTRACT NAS 5-22325

TABLE OF CONTENTS

ABSTRACT

The potential for monitoring ice by imaging radar on the Great Lakes has been demonstrated, but other applications of radar to monitoring of ice, for instance in small lakes and ponds of hydrologic significance, remains to be explored. Although ice-covered rivers appear in numerous radar images, no systematic study of the river-ice monitoring problem has yet been made. The only frequencies studied in the Great Lakes experiments have been in the L- and X-bands, with most measurements in the latter band. No systematic study has been made of the effect of angle of incidence, polarization, or resolution. Clearly considerable experimental work is needed in this area. A theoretical model has been developed for sea ice, but only theory-based inferences have been used to describe radar-return from lake ice.

The formation of lake ice is reviewed with its implications for, and some measured data for, the electrical properties. At the lower frequencies penetration in ice should be great enough so that most of the return probably comes from the bottom of ice in the Great Lakes. Suggestions for ice-monitoring radar system parameters are made, but they are based largely on conjecture from the physical and dielectric characteristics of the ice. More important at this stage are the recommendations for a research program.

Radar Monitoring of Lake/River Ice -- State of the Art

by
S. K. Parashar

1.0 INTRODUCTION

The current state of the art in monitoring lake and river ice by the use of a radar is presented here on the basis of a thorough review of the existing literature. The present interest in the use of radar systems to monitor lake and river ice was primarily developed because of a real need to extend the Great Lakes shipping season into the winter months. The feasibility of achieving this depends to a large extent on making improvements in the ice information gathering techniques. It is important that quick, accurate, and comprehensive information about the position, extent, and relative thickness of ice cover be made available to shippers on a timely basis so that shipping routes for navigation may be optimized. This requires repeated, and in some cases daily, reconnaissance of the ice cover. In view of the tremendous areal extent of the ice cover, the repeated and timely surveillance can be only provided by means of automated remote sensing techniques. It is in this regard that the all-weather, day/night operational capability and broad aerial coverage provided by a Side-Looking Airborne Radar (SLAR) is seen to be of great potential utility in the ice mapping.

Besides a comprehensive review of the past radar measurements of lake and river ice, a section on the formation of lake and river ice is included and the physical and electrical properties of ice which help determine the radar return are given. This will not only help in understanding the nature of radar return from ice but also help in explaining the experimental measurements. In the end an attempt is made to specify optimum parameters for an operational ice surveillance system on the basis of past experimental results. Recommendations are made on the need to conduct future experiments and on the design and requirements of these experiments.

2.0 FORMATION OF LAKE/RIVER ICE

The formation of ice depends primarily on the surface salinity, the vertical distribution of salinity, and the depth of water. The amount of salinity present determines the temperature of maximum density. In water with a salinity of less than 24.7 $^{o}/_{oo}$

the temperature of maximum density lies above the freezing temperature. The freezing temperature of water decreases less rapidly than the temperature of the maximum density, with increasing salinity. The temperature of maximum density in pure water is +3.98° C. Both the temperatures, of freezing and maximum density, are the same at -1.33° C at a salinity of about 24.7 °/oo. Cooling of a layer of water with a salinity of less than 24.7 °/oo causes an increase in the density of water at the surface resulting in free convection. With continued cooling this convection continues until the complete convective column reaches the temperature of maximum density for that particular salinity (14). The convection stops at this time. Further surface cooling, without mechanical mixing, creates a stratification in a very thin stable surface layer of low density where ice formation rapidly begins when the temperature of the freezing point is reached. Lake or river water is of considerable less salinity than 24.7 °/oo.

The formation of ice at the surface begins earlier over shallow depths than over deeper water bodies under similar conditions (5). In the fall lake ice normally forms first, then river ice, and finally sea ice. Both lake and river ice are essentially fresh water structures whereas sea ice is quite salty. The amount of salt present in ice depends on the salinity of the water from which it is formed and is always less than the original water salinity. Ice formation in the rivers is affected by the complete vertical mixing of heat as the result of turbulence.

The salinity of the water does not affect the formation of the initial ice cover once the water starts to freeze. The amount of turbulent mixing of the water in the freezing layer is the determining factor in the formation of ice cover. Thus, factors such as wind, current, and the intensity of cooling are important in influencing the ice formation. Under calm conditions, the initial ice growth starts after water has been supercooled slightly. The first crystals to form are minute spheres of pure ice and as these grow they rapidly change their shape to circular disks (14). In fresh water these disks attain a maximum diameter of 2 to 3 mm which depends on supercooling. The disk form changes to dendritic hexagonal stars at some critical diameter of about 2 to 3 mm in fresh water. This critical diameter appears to decrease with increasing salinity. The stars grow rapidly across the surface of calm lake water until they overlap and freeze together.

Surface needles are common during the initial freezing of fresh water and are formed when a disk becomes inclined at an angle to the water surface. Subsequent growth is in the form of long thin needle-like crystals. These crystals vary considerably

in size and needles up to 4 m in length and vertical crystals up to 0.7 m in diameter are observed (14). Thus, during calm conditions the initial lake ice skim is composed of an open polygonal network of surface needles inclined at some angle from the vertical and in between areas are occupied by the approximately vertical star-like crystals.

Some turbulence during initial ice formation introduces more nuclei into the area of active freezing so that the initial crystals are mixed throughout a depth of up to several meters. Extensive discordal growth is favored and in rivers these discords and needle-like ice fragments are referred to as frazil ice. Irregular structures are formed when these frazil crystals freeze together. Snow falling on the water surface, during calm conditions, just prior to and during initial freezing conditions also helps in the formation of similar crystal aggregates. Ice known as pancake and slush is formed because of packing of ice crystals due to wave motion and the general motion of the aggregates against one another. The thickness of initial ice cover when a slush layer congeals is usually several centimeters. Sheet ice will develop beneath the pancakes and slush ice once a composite ice sheet is formed between the pancakes. It is difficult sometimes to distinguish slush ice from infiltrated snow ice which is formed because of abundant snowfall.

After the initial continuous skim of ice is formed, a transition layer is produced in which a change towards preferred growth orientation of ice crystals is seen. The favored orientation can range from horizontal to vertical. The ice below the transition layer has all the characteristics associated with a "columnar" structure. This columnar zone has a strong crystal orientation and a gradual increase in average grain size as the distance from the surface or the cold source increases. Several characteristics and features such as air bubble layering can be seen in the vertical sections of columnar zone. The shape of the air bubbles is usually tubular and elongated parallel to the growth direction. In lake ice, a pronounced intra-crystalline substructure, which usually forms parallel to the growth direction and has a similar appearance to so called striation boundaries in metals, can be seen.

After the formation of initial ice skim, both lake and river ice usually grow with a planar solid/liquid interface. It is pointed out by Weeks and Assur (14), that the variations in the properties of lake and river ice with changes in temperature should be caused primarily by variations in the properties of pure ice and not by any changes in the relative amount of solid, liquid, or gas present in the ice sample.

2.1 Physical Properties

Both lake and river ice consist of pure ice crystal matrix in which air bubbles are included. The ice may also contain certain forms of solid impurities and liquid inclusions depending on the state and purity of original water and the conditions prevalent at the time of ice formation. The properties of lake and river ice will be primarily those exhibited by pure ice. It is possible to classify naturally-occuring fresh water ice into two major categories on the basis of its formation and growth: (1) ice which grows parallel to the direction of heat flow is called secondary ice; (2) ice which forms on top of the secondary ice, for example, as the result of the flooding of the snow layer, is termed superimposed ice. The secondary ice can be further classified into several ice types on the basis of age and thickness and the way it is formed. From the point of view of remote sensing, frazil ice and columnar ice are probably most interesting (13). As pointed out earlier, frazil ice is formed from an agglomeration of ice particles which have been formed in supercooled turbulent water and can be several centimeters thick. Columnar ice is formed in calm water or under an already existing ice cover, such as frazil ice.

It is the physical properties of ice such as amount and nature of impurities, air bubbles, cracks, density, and temperature which determine the electrical properties. The radar return from lake and river ice depends on the surface roughness at the wavelength scale and the subsurface structure.

2.2 Electrical Properties

The radar return from lake and river ice, as from other surfaces, is determined by the electrical and physical properties of ice. The electrical properties depend on physical properties. The electrical properties of ice of interest are its dielectric behaviour such as dielectric constant and conductivity as a function of frequency and temperature.

The electrical properties of fresh water or pure ice have been investigated by many workers and are quite well established. An overall review of literature on electrical properties of fresh water ice presented by Evans (4). As liquid water changes its physical state into ice, its dielectric properties change significantly. The most interesting properties of pure ice are its high static dielectric constant (about 100) and its

long relaxation time (about 10^{-4}). For frequencies much greater than 1 MHz, the dielectric constant drops to about 3. Most workers have investigated the large dielectric dispersion in pure ice. In general, measurements of contemporary workers have a good correlation with each other and with the Debye equation. The Debye equation for dielectrics is based on polar molecules having a single relaxation time and this relaxation form is fairly common in solids and liquids.

The dielectric behaviour of ice and water as a function of frequency is given in Figure 1. Both ice and water traverse in first approximation a simple Debye relaxation spectrum. In the dispersion region the dielectric loss goes through a maximum and the dielectric constant falls off. The separation in the relaxation spectra of ice and water is approximately six decades of frequency (6). The dielectric loss of water and ice changes drastically by the presence of salts whereas the dielectric constant does not alter as much. Salts add free charge carriers and thus increase the conductivity. Thus, the electrical properties of sea ice which contains salt are significantly different from those of pure ice, and lake or river ice is more like pure ice.

Both the relaxation time and the static dielectric constant of ice are temperature dependent. Between a frequency of 1 MHz and the far infra-red region there is no absorption band in the spectrum of ice. The relative permittivity (dielectric constant) from the measurements made by different workers and compiled by Evans (4), is shown in Figure 2. The code letters identify the individual authorities along with the temperature, and other remarks about the measurements. The differences in the measurements can be attributed to differences in the temperatures and densities of the ice samples.

A scatter plot of the experimental results of dielectric constant obtained by various samples of fresh ice as a function of temperature at 10 GHz is shown in Figure 3. Statistically the value of relative dielectric constant was found to be $3.14 \pm 1.4\%$, which concurs with the measurements made by other workers (13). For fresh (tap) water ice, the measurements in the 26.4 to 40 GHz frequency range indicate a value of relative dielectric constant of $2.92 \pm 2\%$.

The variation of loss tangent with frequency for ice as compiled by Evans (4) is presented in Figure 4. The quantity plotted vertically is $\log_{10}(f \tan \delta)$ where f is the frequency in MHz and $\tan \delta$ is the loss tangent or $\epsilon''_r / \epsilon'_r$ (imaginary part of complex permittivity divided by the real part).

The loss tangent of fresh ice at 10 GHz as obtained by Vant et al (13) was of the order of 20×10^{-4} (0° C to -35° C). Lamb (13) gives a value of 12×10^{-4}

(0° C), Cummings (13) 27×10^{-4} (0° C) to 6.5×10^{-4} (-18°C), and von Hippel (13) 7.0×10^{-4} (-12° C).

The presence of impurities in small quantities may have some effect on the dielectric properties. This effect may be significant depending on the amount and the nature of impurities.

3.0 RADAR RETURN FROM ICE

The radar scattering from lake and river ice is a result of complex interaction of the electromagnetic field with the ice profile. The average power returned by each boundary (air-ice and ice-water boundary) is partly determined by the complex permittivity and the surface roughness. In addition subsurface structure may also have some effect on the radar return. A perfectly smooth surface gives return only in the specular direction where angle of incidence is equal to angle of reflection. With a very rough surface, the scatter is almost uniform in all the directions including the source. For the slightly rough surface most of the incident energy is scattered in the direction near the specular direction. The surface roughness is defined on the incident wavelength scale. For a surface to be defined as smooth, the surface variations should be much smaller than one wavelength, perhaps by an order of the magnitude. Thus, a surface which is smooth at one frequency may not be smooth at a higher frequency. The same surface will appear rougher as the wavelength of the incident energy is decreased.

In addition to surface roughness, the electrical properties of the medium also play an important part. The complex permittivity (the real part is the dielectric constant and the imaginary part can be expressed as a loss tangent) not only determines the amount of energy which is scattered or reflected but also determines the degree of penetration of incident electromagnetic energy. The magnitude of complex permittivity determines the amount of energy scattered or reflected and the loss tangent determines the attenuation in the medium and thus the skin depth and the degree of penetration. For higher values of the loss tangent, the attenuation is greater and hence the skin depth smaller. By selecting a value of 3.15 for dielectric constant and 10×10^{-4} for loss tangent, the skin depth for ice can vary linearly as function of frequency from about 100 cm at 1 GHz and 10 cm at 10 GHz to 1 cm at 20 GHz.

Thus, the choice of the frequency determines the depth of penetration and thereby influences the contributions made by the ice-water interface and the effect of sub-

surface structure. The contribution to radar return from surface roughness is also dependent on frequency.

4.0 STATE OF THE ART

The present state of the art in the radar measurement of lake and river ice can essentially be obtained by conducting a thorough review of the existing literature, and this is the intent and purpose of this section.

Most of the past research efforts in the applications of radar in monitoring ice have been devoted to sea ice. The investigations into the ability of radar to monitor lake and river ice have been rather limited until quite recently. This is partly because of the fact that it is felt that the knowledge about sea ice is of greater practical utility and global interest than the knowledge about lake ice which is of regional value. It is only recently that interest has been developed in investigating the potential of radar in monitoring lake and river ice.

During February and March, 1971, an attempt was made by United States Coast Guard to acquire some SLAR (Side-Looking Airborne Radar) imagery in the Mackinac-Sault Ste. Marie region of the Great Lakes. The radar imagery was obtained with an AN/DPD-2 (Modified) Philco-Ford SLAR operating at 16.5 GHz. In addition to SLAR imagery, vertical aerial photographs in the 9 X 9 inch format were also obtained of certain areas. This was done so that radar imagery could be correlated with the aerial photographs. It was shown then by Photographic Interpretation Corporation in a report prepared for U.S. Coast Guard (11) on the analysis of the data that radar imagery is valuable for the interpretation of lake ice. It was possible to detect, delineate, and describe several lake-ice types through a detailed, systematic study of the available imagery. This was accomplished even though there was lack of information available at that time concerning the various basic categories of lake ice types and their parameters (e.g., thickness, age, and strength). At Ku-band no apparent detrimental masking effect was found by snow cover of lake ice. Some instances of probable penetration of snow cover by radar signals were observed and described. No snow features identifiable as such were detected. Some distinct patterns on the radar imagery were attributed to snow, ice ridges, and mounds on the lake ice surface. It was possible but difficult to describe lake ice patterns and determine relative thickness.

The same data were examined by Raytheon Company in a report prepared for

U.S. Coast Guard (12). It was pointed out that identification of the various ice types was accomplished to the maximum extent possible. It was possible in certain instances to identify new ice types with the aid of complementary photography. Slush, frazil, and grease ice sometimes were not differentiated on lake ice imagery. It was not possible generally to separate young ice into dark gray or gray-white types; these had to be considered one unit. It was only possible to separate dark nilas and light nilas with the aid of aerial photographs. Not enough ice rind was found on the SLAR imagery to arrive at definite conclusions for discrimination. A glossary of ice terms generally used is provided by Dunbar (3).

Winter ice, considered to be of "medium" thickness, was interpreted with relative ease. It was pointed out that even qualitative thickness could not generally be determined with SLAR to any degree of confidence. In certain cases, winter ice appeared to be thicker, and if the surrounding features and collateral data supported the assumption, such ice was termed "thick" winter ice. Sometimes, clues to relative ice thickness were provided by the crack system. Angular cracks implied thinner ice. This technique is not a reliable one.

It was pointed out that the masking effects of snow cover on lake ice tended to complicate the identification of ice types. As confirmed by aerial photographs, almost all of the ice having a continuous snow cover was winter ice. Still other variables are introduced by thin and/or discontinuous snow cover which has to be considered in the identification. It was recommended that the effects of such lesser amounts of snow cover be analyzed further under controlled conditions so that these influences on the SLAR imagery may be understood and isolated.

A series of X-band SLAR images were obtained by NASA Lewis Research Center (7) to show the development and disintegration of the entire ice cover on Lake Erie during the winter of 1972-73. The accurate correlation of radar responses with ice conditions was established through simultaneous ground truth observations and ERTS-1 photography. Motorola AN/APS-94C real aperture SLAR system operating at 9.2 GHz frequency with horizontal transmit and receive polarization was used to acquire imagery. It was possible to identify ice types such as brash, pancake, and related forms because of their brightest return. It was pointed out that these ice types give brightest return simply due to the large vertical cross-section presented by their edges. Thus, surface roughness of ice was considered to play a dominant role in the radar return. Because of the penetration of the wave the roughness of the ice-water interface may also contribute strongly to the radar return. Only in the case of fast ice were there any indications of

volume scattering. It was not possible to discriminate unfractured ice from open water because (it was felt) smooth clear ice lacks sufficient defects to backscatter enough radiation to be detected. Most of the returns in this study were near grazing incidence, so the effect of steeper angles cannot be evaluated.

During the 1973-74 winter, measurements were made with the 2-frequency (X-band and L-band) synthetic-aperture system of Environmental Research Institute of Michigan (2). Two sites near the entrance to Great Lakes were studied: Whitefish Bay on Lake Superior and the Straits of Mackinac between Lakes Michigan and Huron. Both HH (horizontal transmit, horizontal receive) and HV (horizontal transmit, vertical receive) images were produced in each band. The systems have resolutions much finer than for other reported measurements.

Smooth black ice with embedded brash ice gave weak returns and rough brash ice gave strong HH returns at both frequencies. In one relatively smooth area moderate return occurred only on the L-band (HH, HV) images. One area of poorly-developed ice foot showed only on X-band (HH, HV) images. In most cases pressure ridges showed up on all images, but one could only be detected on the X-HV image.

Interpretations suggested that much of the scatter was from the lower surface of the ice, particularly at L-band.

As is clear from above, the radar measurements from lake ice are rather limited and there are no measurements available for river ice. Furthermore, the past results are inconsistent. The only consistency which can be seen from different studies is that radar may very well be a valuable tool in discriminating and identifying lake ice. It is not possible to measure ice thickness directly, but it can be inferred by dividing ice into types on the basis of thickness. There is a lack of qualitative and quantitative data available which can help in relating ice thickness and/or type to radar backscatter. More research should be conducted with a view not only to explore the potential and prove the capability of SLAR in monitoring lake ice but also to provide enough reliable information for the design of future operational systems.

5.0 RECOMMENDATIONS

To be able to design an optimum operational radar system for ice monitoring, the effect of frequency, polarization, and angle in discriminating ice types has to

be clearly understood. This understanding of the nature of radar return can be obtained in part by collecting qualitative data corresponding to different operating parameters and then establishing the optimum ones. This, however, requires much data gathering and the time required to accomplish this and the cost may be prohibitive.

Another approach is to formulate an analytical model which will help in computing the radar return corresponding to different operating parameters and ice types and conditions. For this case, the qualitative data with excellent "ground-truth" need only be acquired for selected parameters so that the validity of the theoretical model can be established. On the basis of this model optimum parameters can then be specified. Such a theoretical model has been formulated for sea ice (10) and it shows reasonably good agreement with the experimental results. The good point in the favor of a theoretical model is not only that it helps in explaining and understanding the nature of radar return but also it separates out the effect of surface roughness from other effects. Thus, the model helps in establishing the relative contributions from surface roughness and the dielectric properties.

In addition to establishing the frequency, polarization, and angle, the other parameter which needs to be established is the size of the resolution cell. It may be possible to discriminate ice types better with a moderate resolution cell size than with fine or coarse size. It is not suggested here that only a single frequency, polarization, and range of angles is suitable for ice discrimination. It may very well be that a combination of frequencies, polarization, and ranges of angles provide better information in identifying ice types.

The other parameters which need to be specified are the sensitivity and the dynamic range of the radar return. This can be achieved by acquiring radar scatterometer measurements over varying ice conditions. Radar scatterometers by design are calibrated systems and they measure the radar backscatter coefficient or radar scattering cross-section per unit area. Radar scatterometers, by measuring variation of the radar scattering coefficient, σ^{o}, with angle, frequency, and polarization, permit more detailed observation of radar scattering behavior than radar images (9). Almost all the radar imagers in operation today are uncalibrated systems operating largely near grazing incidence. The gray tone or density on a radar image is proportional to the power received which in turn is directly proportional to the radar scattering coefficient. Thus, by establishing the sensitivity and the dynamic range of the radar backscatter coefficient the corresponding parameters for a radar imager

can be specified. No radar scatterometer data is avilable for lake and river ice.

Though it is a difficult and a dangerous task to specify parameters for future operational systems on the basis of meagre data available, yet an attempt is made below to infer these parameters. The specifications recommended here are by no means optimum or the best or the only ones possible.

1) Frequency

Past measurements have only been made at two frequencies: X-band and Ku-band plus a very few of L-band. It does not appear that one high frequency is better than the other, though more ice types were identified on Ku-band imagery. In certain instances the snow masking effects were detrimental to ice identification but in general Ku-band signals do appear to penetrate dry snow.

The two parameters of interest in ice monitoring are the relative ice thickness and the surface roughness. Both of these parameters help determine the mechanical properties such as strength and also help in establishing the drift patterns and climatological conditions from the corresponding mathematical theoretical models. The knowledge of ice thickness and also the presence of open water helps in determining the optimum navigational route.

The choice of frequency or frequencies should then be made by bearing in mind the above mentioned parameters of interest namely, ice thickness and roughness. A signal at a lower frequency will generally be able to penetrate more as compared to a higher frequency. Thus, radar return at a lower frequency will be relatively more influenced by the ice-water boundary. Moreover, the contribution made by the roughness is also dependent on the frequency. The same surface will appear rougher with an increase in frequency.

The frequency or frequencies should also be selected on the basis of achievable resolution cell size with a reasonable size antenna.

By keeping these factors in mind, a choice of two frequencies, one at L-band around 2 GHz and the other at Ku-band around 16 GHz seems to be appropriate. If only one frequency is required, X-band around 10 GHz seems to be more feasible. The signals at the L-band will be able to penetrate more and thus the radar return will be influenced to a greater degree from the ice-water boundary. This may help in differentiating thicker types of ice. Also L-band signals will be effected more by the large scale roughness and may very well provide qualitative and quantitative information about the roughness such as pressure ridges. Ku-band signals will be

able to penetrate less and will be more influenced by the small scale roughness. This may help in differentiating thinner, very rough types of ice such as brash.

The choice of X-band is made as single frequency simply because conceivably it will have the best of both. It will be able to penetrate a little and also be influenced by medium scale roughness. To achieve moderate or fine resolution at these frequencies, especially at L-band, a synthetic aperture antenna is required even for aircraft systems. SAR is required for spacecraft systems at any frequency.

2) Polarization

There does not appear any difference between two like polarizations (HH - horizontal transmit, horizontal receive; VV - vertical transmit, vertical receive) in their ability to distinguish ice types, but cross-polarized signals may be effective in discriminating ice types as is evident in the case of sea ice (10). Thus, one like polarization (HH or VV) and one cross-polarization (HV or VH) is recommended, but the latter is based largely on conjecture.

3) Incidence Angles

The selection of incidence angles should be based on their ability to distinguish ice types. No such information is available from the past measurements. Since one of the aims in ice monitoring is the location of navigational open water, the choice of angles may very well be based on this criterion. Open water can generally be detected by operating well away from the vertical because as a comparitively smooth surface it does not give any return at near grazing angles and thus appears black. Hence a range of angles from about 30 to 75 degrees is proposed. Since some of the smooth ice categories also give low return, these angles may be less suitable than they are for sea ice.

4) Resolution Cell Size

This selection should be based on two criteria. One is the minimum resolution cell size needed to identify an ice type and the minimum size floe which needed to be identified. The other is the minimum size of open water lead which is adequate enough for the passage of a ship. For lack of better information available, a moderate size of 20 to 30 meters is proposed. Note that this is finer than that of either DPD-2 or APS-94C.

5) Dynamic Range

No data are available on which selection can be based. On the basis of sea ice data (10), a dynamic range of 40 dB at above mentioned operating angles should be more than adequate. A dynamic range of less than this may actually be required.

6) Sensitivity

Again there is a lack of available information; in fact there is none! On the basis of sea ice data (10), it should be possible to detect a minimum radar scattering coefficient, σ^o, of about -20 dB for like polarization and -50 dB for cross-polarization. The system should be sensitive enough to record and distinguish variations of 0.2 dB and these variations should be reflected in gray tones on the radar imagery. Some evidence indicates that sensitivity better than for sea ice would be useful.

7) Frequency of Coverage

During winter time a coverage every day may be needed to find optimum shipping routes on the lakes. Coverage for rivers may also be needed daily at times of ice-jam build up, but weekly coverage may be sufficient at other times.

6.0 CONCLUSIONS

It is evident from the above that SLAR is potentially a valuable tool in monitoring lake and river ice. Before an optimum system of general utility can be designed more research, both experimental and theoretical needs to be conducted. A need exists to collect more qualitative and quantitative data with a view of establishing optimum operating parameters and understanding the nature of radar return from ice. These experiments should be carefully designed and properly organized so that maximum information from them can be derived. The need to collect good "ground truth" data in terms of ice thickness, surface roughness, temperature, and electrical parameters should be borne in mind. The experiments should be conducted in different parts of the season so that the effect of temperature, growth, and melt can be properly evaluated. The measurements corresponding to different frequencies, polarizations, range of angles, and resolution cell size should be made for both lake and river ice. A "ground-based" radar spectrometer offers more potential for these measurements than any airborne system.

A theoretical model of wave scattering from fresh-water ice needs to be formulated. To test this model properly, measurements under semi-controlled conditions have to be made at selected parameters. To properly correlate these measurements with ice types a good system to collect the necessary "ground truth" information must be set up. These measurements can be made by a ground based scatterometer operating at a number of frequencies. Later airborne scatterometer

measurements may be helpful to establish dynamic range and sensitivity.

The effect of snow on radar return needs to be evaluated more thoroughly. Furthermore, lake and river ice should be divided into standard categories as has been done in the case of sea ice. Relative thickness should be associated with each ice type.

Fine-resolution images should be produced to assist in establishing required resolutions. These may be degraded by different amounts, and the degraded images evaluated by interpreters to set critical levels for different purposes.

REFERENCES

1. Bryan, M. L. and R. W. Larson, "Applications of Dielectric Constant Measurements to Radar imagery Interpretation," Second Annual Remote Sensing of Earth Resources Conference, University of Tennessee Space Institute, March 26 - 28, 1973.

2. Bryan, M. L. and R. W. Larson, "The Study of Fresh-Water Lake Ice Using Multiplexed Imaging Radar," Journal of Glaciology, Vol. 14, No. 72, 1975.

3. Dunbar, Moira, "A Glossary of Ice Terms (WMO Terminology)," Ice Seminar, Special Volume 10, The Canadian Institute of Mining and Metallurgy, pp. 105 - 110, 1969.

4. Evans, S., "Dielectric Properties of Ice and Snow - A Review," Journal of Glaciology, vol. 5, pp. 773 - 792, 1965.

5. Groen, P., The Waters of the Sea, D. Van Nostrand, Co., Ltd., London, 1967.

6. Hoekstra, P. and . Cappillino, "Dielectric Properties of Sea Ice and Sodium Chloride Ice at UHF and Micro-Wave Frequencies," Journal of Geophysical Research, vol. 76, no. 20, pp. 4922-4931, July, 1971.

7. Jirberg, R. J., R. J. Schertler, R. T. Gedney, and H. Mark, "Application of SLAR for Monitoring Great Lakes Total Ice Cover," NASA TMX-71473, NASA Lewis Research Center, Cleveland, Ohio, 44135, Dec. 1973.

8. Larrowe, B. T., et al., "Fine-Resolution Radar Investigation of Great Lakes Ice Cover," Final Report, Willow Run Laboratories, University of Michigan, Jan. 1971.

9. Moore, R. K., "Radar Scatterometry - An Active Remote Sensing Tool, " University of Kansas Center for Research, Inc., CRES Technical Report 61-11, Remote Sensing Laboratory, Lawrence, Kansas, April, 1966.

10. Parashar, S. K., "Investigation of Radar Discrimination of Sea Ice," (Ph.D. Thesis) University of Kansas Center for Research, Inc., CRES Technical Report 185-13, Remote Sensing Laboratory, Lawrence, Kansas, Dec. 1973.

11. United States Coast Guard, "Interpretation of Winter Ice Conditions from SLAR Imagery," Report No. DOT-CG-14486-1A, Department of Transportation, Office of Research and Development, Washington, D. C., 20591, Feb. 1972.

12. United States Coast Guard, "Analysis of SLAR Imagery of Arctic and Lake Ice," Report No. DOT-CG-14486-A, Department of Transportation, Office of Research and Development, Washington, D. C., 20591, Feb. 1972.

13. Vant, M. R., R. B. Gray, R. O. Ramseier, and V. Makios, "Dielectric Properties of Fresh and Sea Ice at 10 and 35 GHz," Journal of Applied Physics, vol. 45, No. 11, pp. 4712-4717, November 1974.

14. Weeks, W. F. and A. Assur, "Fracture of Lake and Sea Ice," Research Report 269, Cold Regions Research and Engineering Laboratory, Hanover, New Hampshire, September 1969.

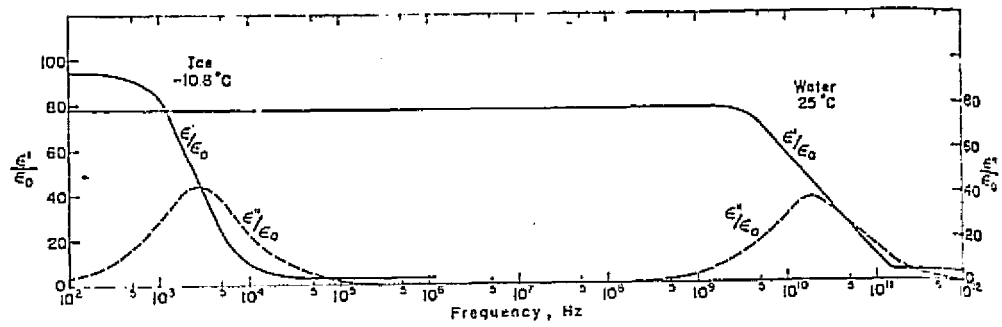

Figure 1. The dielectric behavior of ice and water as a function of frequency (Hoekstra and Capillino (6)).

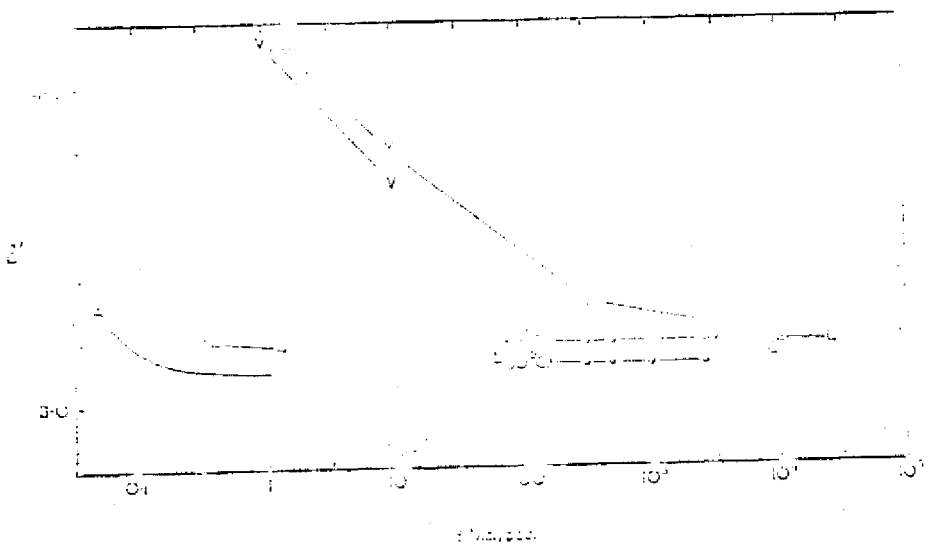

Figure 2. Relative permittivity of ice (ordinates) versus logarithm of radio-frequency (abscissae) (Evans (4)).

L: Lamb (1946) and Lamb and Turney (1949) - 5° C at low frequencis, 0° to -190° C at high frequencies: distilled water.
C: Cummings (1952) - 18° C. Distilled water and melted snow.
A: Auty and Cole (1952) - 10° C. Conductivity water: ice free from stress.
V: Von Hippel (1954) - 12° C. Conductivity water: ice not annealed.
Y: Yoshino (1961) - 18° to -36° C. Antarctic ice, not annealed, density 0.91 g/cm^3.
W: Westphal (private communication) - 5° to -60° C., annealed Greenland ice, density 0.90 g/cm^3.

14. Weeks, W. F. and A. Assur, "Fracture of Lake and Sea Ice," Research Report 269, Cold Regions Research and Engineering Laboratory, Hanover, New Hampshire, September 1969.

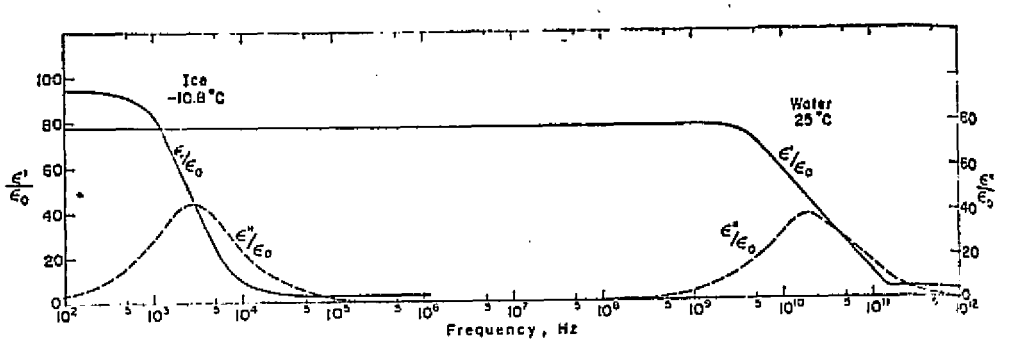

Figure 1. The dielectric behavior of ice and water as a function of frequency (Hoekstra and Capillino (6)).

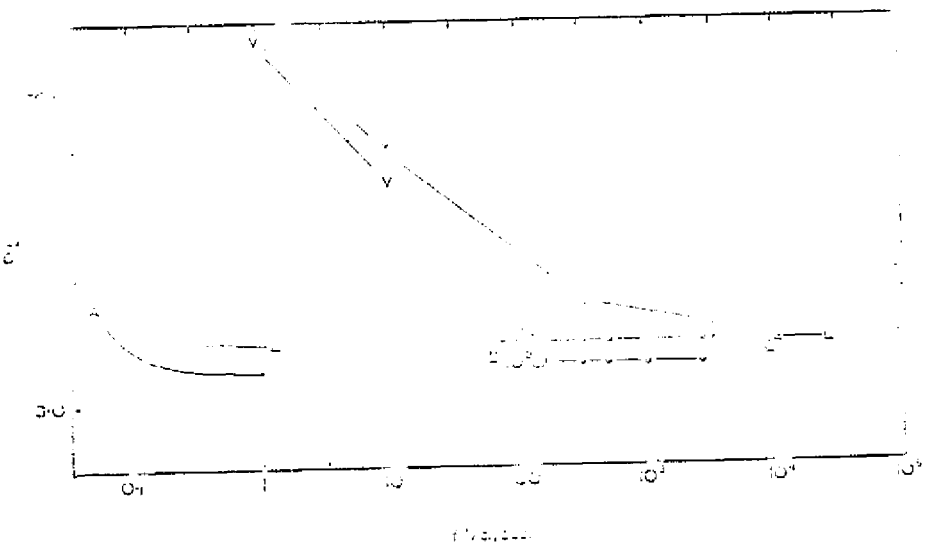

Figure 2. Relative permittivity of ice (ordinates) versus logarithm of radio-frequency (abscissae) (Evans (4)).

L: Lamb (1946) and Lamb and Turney (1949) - 5° C at low frequencis, 0° to -190° C at high frequencies: distilled water.
C: Cummings (1952) - 18° C. Distilled water and melted snow.
A: Auty and Cole (1952) - 10° C. Conductivity water: ice free from stress.
V: Von Hippel (1954) - 12° C. Conductivity water: ice not annealed.
Y: Yoshino (1961) - 18° to -36° C. Antarctic ice, not annealed, density 0.91 g/cm^3.
W: Westphal (private communication) - 5° to -60° C., annealed Greenland ice, density 0.90 g/cm^3.

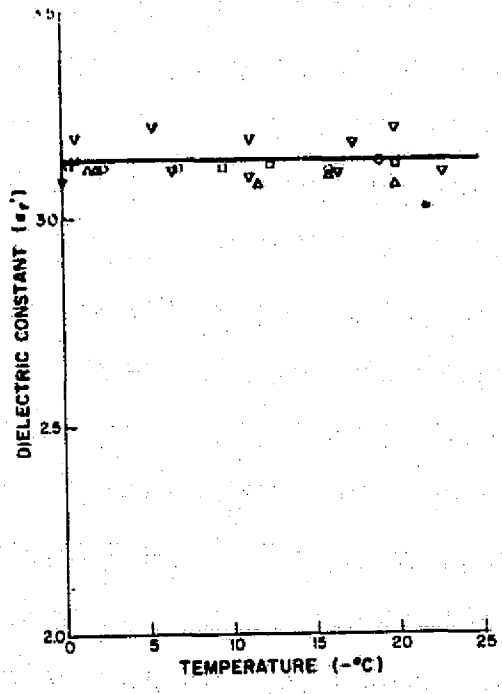

Figure 3. Results of free-space measurements of dielectric constant of pure ice (Vant, et al., (13)).

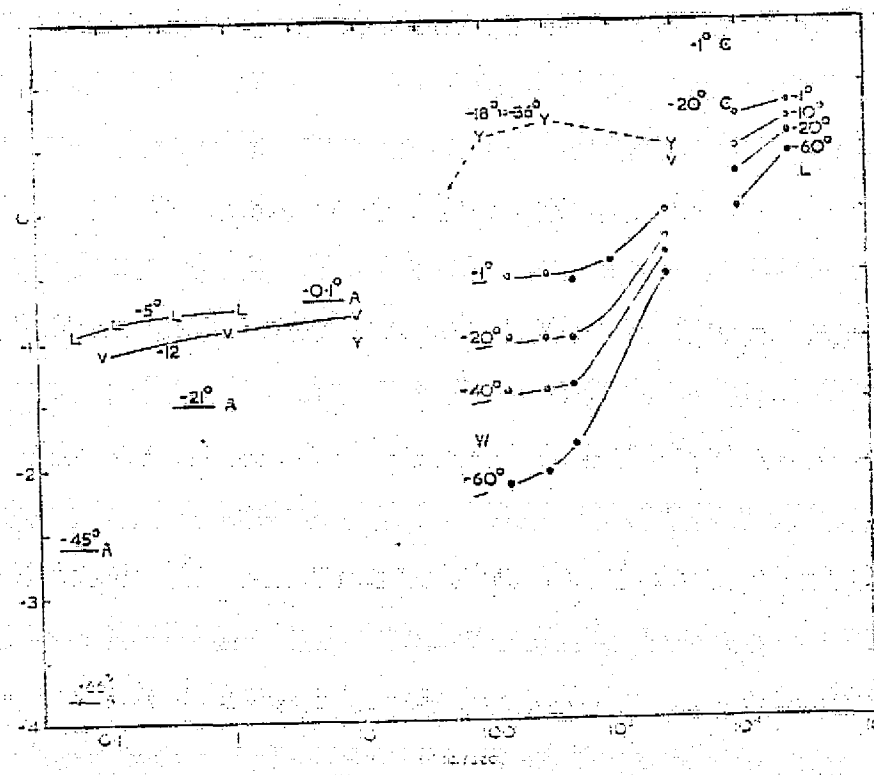

$\log_{10}$ (f tan δ)

Figure 4. Loss tangent of ice versus radio-frequency. The quantity plotted vertically is $\log_{10}$ (f tan δ) where f is the frequency in Mc./sec. On the high-frequency tail of a relaxation spectrum this quantity is constant: it has the further useful property that the attenuation of a radio wave (measured in dB./m.) passing through the medium is directly proportioned to f tan δ. Temperatures are marked in °C. (Evans, (4)). (key on following page).

L: Lamb (1946) and Lamb and Turney (1949). Distilled water, ice not annealed.

C: Cumming (1952). Distilled water, tap water, and melted snow (no observable difference).

A: Auty and Cole (1952). Conductivity water, ice free from stress. Limiting values plotted arbitrarily at 1,000 times the relaxation frequency.

V: Von Hippel (1954). Conductivity water, ice not annealed.

Y: Yoshino (1961). Antarctic ice core samples, not annealed, density 0.91 g./cm.^{3}

W: Westphal (private communication). Greenland ice, annealed, density 0.90 g./cm.^{3}

Approximate temperature coefficients below ~ 10° C.

1 Mc./sec. 0.05 per °C. in log tan δ = 12% per ° C. in tan δ (from Auty and Cole).

100 Mc./sec. 0.025 per °C. in log tan δ = 6% per °C. in tan δ (from Westphal)

10^4 Mc./sec. 0.01 per °C. in log tan δ = 2.5% per °C. in tan δ (from Lamb)